Climate Risk Management 31 (2021) 100272

Contents lists available at ScienceDirect

Climate Risk Management

journal homepage: www.elsevier.com/locate/crm

Modelling hydrological processes under climate change scenarios in the Jemma sub-basin of upper Blue Nile Basin, Ethiopia

Gebrekidan Worku [a,*], Ermias Teferi [b,d], Amare Bantider [c,d], Yihun T. Dile [e]

[a] Department of Natural Resources Management, Debretabor University, Ethiopia
[b] Center for Environment and Development Studies, Addis Ababa University, Ethiopia
[c] Center for Food Security Studies, Addis Ababa University, Ethiopia
[d] Water and Land Resources Center, Addis Ababa University, Ethiopia
[e] College of Agriculture and Life Sciences, Texas A&M University, TX, USA

ARTICLE INFO

Keywords:
Climate Change
Hydrological processes
SWAT
RCP
Jemma
Blue Nile Basin

ABSTRACT

This study examines the response of hydrological processes to different climate change scenarios in the Jemma sub-basin of the Blue Nile Basin. Future near-term (2021–2050) and long-term (2071–2100) climate scenarios were developed from six statistically bias corrected Regional Climate Models (RCMs) under two Representative Concentration Pathways (RCPs) scenarios: RCP4.5 and RCP8.5. The outputs of climate models were used as input to a calibrated and validated Soil and Water Assessment Tool (SWAT) model to assess the impact of climate change on the hydrology of the sub-basin. For a robust hydrologic representation, the SWAT model was calibrated and validated at three River gauging stations and provided an acceptable result. The climate scenarios developed from bias corrected RCMs projected an increase in temperature in all models and a decrease in rainfall in the ensemble mean of the models in the near-term and long-term climate scenarios. Climate change may cause a consistent decrease in surface runoff and total water yield and an increase in evapotranspiration under all climate scenarios. This study recommends water management structures which can conserve water for agriculture and other ecosystem services in the Jemma sub-basin and in other similar areas in Ethiopia.

1. Introduction

Climate change is expected to influence the availability of freshwater resources through changes in evaporation, soil water and relative humidity in the future (Bates et al., 2008; IPCC, 2013). The most significant potential effects of climate change may include increase in frequency and magnitude of droughts and floods and changes in water supplies due to the expected changes in precipitation, temperature, humidity, soil moisture, runoff and other important components of the hydrologic cycle (Bates et al., 2008). For example, a rise in temperature will lead to increased evapotranspiration and in turn, further increases the demand for irrigation water (Wang et al., 2012). On the other hand, the expected increase in intensities of rainfall will lead to higher rates of surface runoff and an increased risk of flood. Such hydrologic changes will impact nearly every aspect of human well-being such as water supply, agricultural productivity and energy production. For instance, globally it was projected that the number of people who face water stress will increase from 12 to 81 million in the 2020 s and from 79 to 178 million in the 2050 s (Arnell, 2004). Thus, in order to support water

* Corresponding author.
E-mail address: gebrwor@dtu.edu.et (G. Worku).

https://doi.org/10.1016/j.crm.2021.100272
Received 21 July 2020; Received in revised form 1 January 2021; Accepted 3 January 2021
Available online 9 January 2021

management under a changing climate, the impact of climate change on fresh water needs to be quantified.

Several studies have been conducted to assess the impact of climate change on hydrological processes and water availability at different spatial scales. For instance, in the Matson Ditch watershed of Indiana, increases in surface runoff and subsurface flow were estimated using bias adjusted GCM simulations under the emission scenarios of RCP4.5 and RCP8.5 (Mehan et al., 2019). On the contrary, a decreases in streamflow, surface runoff, total water yield and soil water storage were projected by the mid-21st century using bias corrected climate models output under A2, A1B and B1 in the Skunk Creek watershed of South Dakota (Mehan et al., 2016). Difference in geographic location and climatic characteristics of the watersheds and variation in emission scenarios may result such contrasting effect of climate change. Similarly, in watersheds of the Upper Blue Nile Basin of Ethiopia, several studies (e.g. Setegn et al., 2011; Adem et al., 2016; Worqlul et al., 2018) have explored the impact of climate change on different water balance components. At regional and global scales Arnell (2004); Elshamy et al. (2009) and others explore the response of hydrologic components to different climate projections. There is difference among studies in using climate model simulations. Some studies directly apply outputs of Global Climate Models (GCMs) and RCMs (e.g. Beyene et al., 2010; Setegn et al., 2011), while others used bias-adjusted and downscaled climate models output before applying for hydrological estimations (e.g. Elshamy et al., 2009; Teutschbein and Seibert, 2012; Liersch et al., 2016; Mehan et al., 2019).

However, the standard procedure of climate change impact assessment include downscaling of GCMs output into regional scales, tailoring (bias correction) of RCMs output, hydrological simulation and analysis of changes exclusively due to climate change (Olsson et al., 2016). When assessing the effects of climate change on water resources, it is also very important to understand the effect of spatial scale. Due to coarse spatial resolution, climate models are characterized by uncertainty to simulate local scale climate variables that are used to fed for hydrological models. For this reason, it is strongly recommended to downscale and bias correct climate models simulation before using for hydrological impact assessment (Teutschbein and Seibert, 2012).

Hydrological simulations using the bias corrected climate models output provide reliable estimate of hydrological components for instance surface runoff, evapotranspiration and water yield than hydrological simulation without bias correction of climate models (Hagemann et al., 2011; Teutschbein and Seibert, 2012; Muerth et al., 2013; Bastola and Misra, 2013). For instance, Fang et al. (2015) has investigated that RCM simulations without bias correction showed large biases of streamflow simulation, while bias corrected RCMs were effective in streamflow simulation. Bias correction has also showed improved performance in simulating rainfall and discharge characteristics (Liersch et al., 2016). However, sometimes bias corrections trigger biases (Maraun, 2012; Wang and Kotamarthi, 2015). In the Canada and the central North America, bias corrected WRF (Weather Research and Forecasting) RCM has showed larger wet bias than the non-bias corrected WRF simulation (Wang and Kotamarthi, 2015). Therefore, it is important to identify appropriate bias correction method and apply bias correction on climate models simulation before using for various applications. It is important, however, to note that there are a relatively limited number of studies in Ethiopia (Elshamy et al., 2009; Liersch et al., 2016; Chaemiso et al., 2016) that incorporate bias corrected RCMs output for climate change impact assessment and climate adaptation decision analysis.

In Ethiopia, the current climate has caused drought, floods, heavy rains and frosts (World Bank, 2006). Among these impacts of climate, drought is the most severe impact of climate change which affect the country frequently (NMA, 2007). There are also various watershed and basin scale studies which account the impact of climate change on the water resource. In the Awash Basin, a decrease in runoff which ranges from 10% to 34% was projected using a single GCM with coarse resolution (Hailemariam, 1999) which could be subject to uncertainty. Taye et al. (2018) has also projected a decrease in water resources in the future period at Awash River Basin using three GCMs from Coupled Models Inter-comparison Project phase 5 (CMIP5). In contrast to the case of Awash River Basin, an increase in surface runoff and total water yield was projected for the 2030 s and 2090 s climate using bias corrected RCM output in the Omo-Gibe River Basin of Ethiopia (Chaemiso et al., 2016). The difference in signals of change on water resources at different basins due to climate change imply the need to investigate hydrological impacts of climate change using appropriate climate change scenarios that could capture local scale climate variables.

In the Upper Blue Nile Basin, there are some hydrological climate change impact studies which apply ensemble of various GCMs (e.g Elshamy et al., 2009; Setegn et al., 2011) and statistically and dynamically downscaled GCMs output (Worqlul et al., 2018; Adem et al., 2016; Mekonnen and Disse, 2016; Dile et al., 2013; Soliman et al., 2009). However, there are limited studies which use bias-corrected outputs of GCMs and RCMs (Elshamy et al., 2009; Liersch et al., 2016) as inputs to hydrological models. There are also studies which use a single emission scenario (Soliman et al., 2009) and different emission scenarios (Worqlul et al., 2018; Adem et al., 2016; Liersch et al., 2016). The findings from these studies provided non-conclusive impact of climate change on hydrological processes. For example, some studies (e.g. Worqlul et al., 2018; Adem et al., 2016; Liersch et al., 2016) simulated an increase in streamflow while others (e.g. Elshamy et al., 2009) simulated a decrease in streamflow. There are also studies existed which projected a nonlinear trend of climate change impact on streamflow (e.g. Setegn et al., 2011). This suggested that there is no conclusive consensus on the impact of climate change on streamflow in the Upper Blue Nile Basin. Thus, it is worthwhile to recognize and characterize the uncertainties of climate change in the basin.

This study was conducted in the Jemma sub-basin of the Upper Blue Nile Basin, which is characterized by frequent drought and extreme temperature and rainfall events (Worku et al., 2018a). The livelihood of the majority of the inhabitants is based on rain-fed agriculture which is frequently affected by climate variability. This suggests that climate change will significantly affect the livelihoods of the smallholder farmers, which warrants detailed climate impact studies to support policy on climate change adaptation. However, there is limitation in integrating climate information and climate adaptation strategies to reduce climate change impacts in Ethiopia (World Bank, 2006; Conway and Schipper, 2011). Thus, this study is important to develop robust hydrological climate impact scenarios for designing optimal climate based hydraulic structures.

This study is also essential to provide climate information generated from different climate change scenarios. To develop climate

change scenarios, bias corrected RCMs rainfall and temperature output under different emission scenarios are essential. Bias correction has been found important because, even though, RCMs are able to capture mean annual and monthly rainfall and distribution of rainfall events, RCMs showed wet bias in the higher elevation (>2700 m above sea level) areas of the Jemma sub-basin (Worku et al., 2018b). This highlights the need to bias adjust RCM simulations before using for hydrological climate change impact assessment. There is no such study in the sub-basin which has assessed the impact of climate change on water availability for agriculture and other services using robustly bias corrected outputs of RCMs. This study, therefore, aims at assessing the impact of different climate change scenarios on the availability of future water resources in the Jemma sub-basin using the Soil and Water Assessment Tool (SWAT) model.

2. Materials and methods

2.1. Description of the study area

Jemma sub-basin is located in the south eastern part of the Upper Blue Nile Basin and has an area of ~ 15,000 km^2 (Fig. 1). It covers ~ 8% of the area and contributes ~ 14% of the total annual flow of Upper Blue Nile Basin (Yilma and Awulachew, 2009). Soil erosion is severe in the sub-basin where it discharges significant amount of sediment to Upper Blue Nile River (Ali et al., 2014). The annual rainfall in Jemma sub-basin ranges between 700 mm and 1400 mm. There are two rainfall seasons in Jemma, summer locally called *Kirmiet* (i.e. June- September) is the main rainfall season and spring locally called *Belg* (March-May) is the small rain season. The temperature in the sub-basin is mild, where the average annual temperature ranges from 9 °C to 24 °C. The elevation in the sub-basin ranges from 1040 m to 3814 m above sea level.

The land use/land cover types in the Jemma sub-basin include agricultural land (56.72%), grazing land (14.64%), bare land (10.45%), shrubland (6.44%), woodland (6.05%) and forestland (1.20%). The remaining land is covered by afro-alpine vegetation, eucalyptus plantations and water bodies. The soil types in the sub-basin include Eutric Vertisols (28.07%), Lithic Leptosols (37.44%), Chromic Lixisols (8.07%), PellicVertisols (6.82), Haplic Luvisols (5.79%), and Haplic Acrisols (6.82). Eutric Fluvisols, Umbric Nitisols and Alic Niti sols cover a small fraction of the sub-basin. The land use/land cover, soil and elevation classes of the sub-basin are presented on Fig. 2.

Jemma sub-basin has several watersheds. Among them, Beressa in the upstream and Robi-Gumero in the middle stream are important where they constitute weather station and hydrological gauge stations. The data from these watersheds were used for

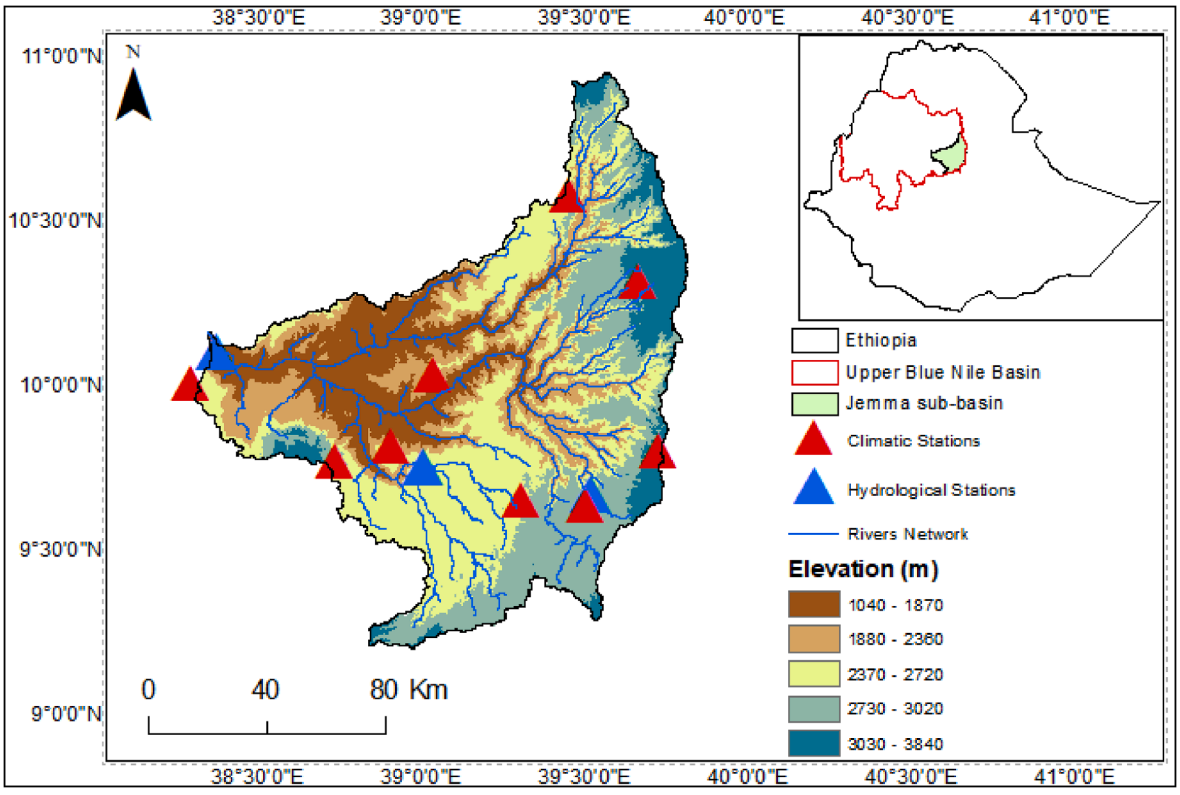

Fig. 1. Jemma sub-basin and distribution of the climatic stations and hydrological gauge stations used for calibration and validation of the hydrological model.

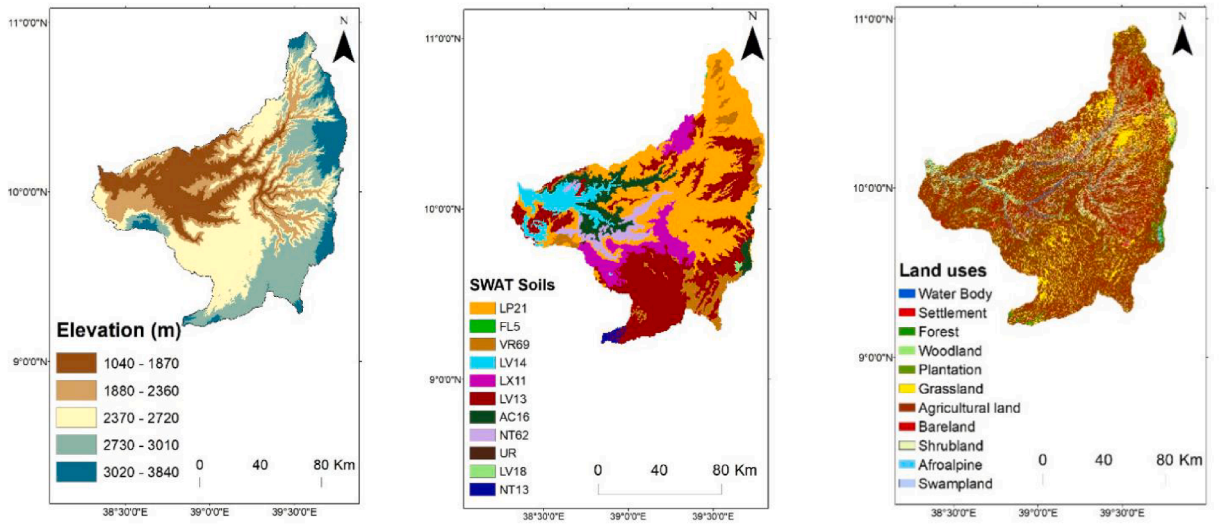

Fig. 2. Elevation, soil types and land use classes of the Jemma sub-basin.

calibration and validation of SWAT model. Beressa watershed is drained by Beressa River and it is the major tributary of Jemma River. This watershed has an area of about 220 km^2 and it is characterized by rugged topography and high elevation which ranges from 2700 to 3650 m above sea level. In this watershed, one climatic station (Debrebirhan) and one hydrological station (Beressa) are located. The baseline climate (1981–2013) mean annual rainfall in the Debrebirhan station of Beressa watershed is 908 mm with a minimum of 649 mm in 1984 and a maximum of 1073 mm in 2007 (Worku et al., 2018a). The main rainfall season is summer (June-September) followed by spring season (March-May). In this watershed, the natural vegetation cover has considerably declined and substituted by planation forest. Soil degradation and water shortage are severe. As a result, the livelihood system of residents has changed from annual crops cultivation to tree planting and livestock production (Amsalu et al., 2007). Eutric Cambisols and Pellic Vertisols are the dominant soil types in Beressa watershed.

Robi-Gumero watershed is drained by Robi River is also a tributary of Jemma River and located in the middle of the sub-basin. The area of this watershed is around 887 km^2. Robi-Gumero watershed is also characterized by rugged topography and elevation ranges from 2300 to 3000 m above sea level. In this watershed, the nearest climatic station is Lemi and the hydrological station is Robi-Gumero gauge station. This watershed is among the areas of the Jemma sub-basin which receives highest amount of annual rainfall. The baseline climate (1981–2013) mean annual rainfall of the Lemi climatic station of Robi-Gumero watershed is 1278 mm with a minimum of 730 mm in 2002 and a maximum of 2459 mm in 2008 (Worku et al., 2018a). The main rainfall season is summer (June-September) followed by spring season (March-May). Agricultural land is the main land use type in this watershed. Pellic Vertisols and Eutric Vertisols are the major soil types in the Robi-Gumero watershed.

2.2. Input data

The SWAT model requires spatial and temporal data to simulate hydrological processes. The spatial data includes Digital Elevation Model (DEM), soil and land cover data, while the temporal data used in the modelling process are the climatic and streamflow data. The DEM data which has a 30 m resolution was obtained from the Shuttle Radar Topographic Mission (SRTM). The DEM data was used to create the basin boundary and stream networks. The slope generated from the DEM data was used to define Hydrological Response Units (HRU) together with the soil and land use data. The soil data was obtained from the Ministry of Water, Irrigation and Electricity of Ethiopian. Soil parameters such as soil saturated hydraulic conductivity, available water capacity, soil texture, etc) are obtained from Water and Land Resources Centre of Ethiopia and from Harmonized World Soil Database (FAO/IIASA/ISRIC/ISS-CAS/JRC, 2008). The land use/land cover data for the year 2008 was derived from Landsat satellite imagery and supervised image classification was done using maximum likelihood algorithm. The land use land cover map was prepared with Kappa (K) statistics and overall accuracy of 0.81% and 83% respectively. Kappa (K) statistics measures the agreement between two images as described by diagonal entries in the error matrix. After the different land use classes were identified, they were redefined according to SWAT land use database code. Thus, the land use/land cover of 2008 was used to represent the land use of the baseline period. All the spatial data were projected to the same projection parameters (i.e. WGS_1984_UTM_Zone_37N).

Baseline climate (1981–2013) daily rainfall, Maximum Temperature (TMAX) and Minimum Temperature (TMIN) solar radiation, sunshine, wind speed and relative humidity of 15 climatic stations of the Jemma sub-basin were obtained from the Ethiopian National Meteorological Services Agency. However, only climate data of nine climatic stations were used in this study. Because these nine climatic stations have data with relatively minimal missing values range from 2% to 17% and adequate years of observation. For climatic stations where there is no observation of solar radiation, sunshine, wind speed and relative humidity, reanalysis dataset i.e Climate Forecast System Reanalysis (CFSR) was used. CFSR is designed based on coupled atmosphere–ocean-land surface-sea ice

system to provide high resolution and best estimate of climatic variables (Saha et al., 2010). These climatic data were used to calculate weather stations statistics which is needed to create SWAT's weather generator input file (Arnold et al., 2012a, 2012b). Daily rainfall, TMAX and TMIN were also used to statistically bias correct RCMs simulation. Daily streamflow data of Beressa (1991–2008), Robi-Gumero (1988–2002) and Jemma (1996–1997) gauge stations was obtained from Ethiopian Ministry of Water, Irrigation and Electricity. These climatic and hydrologic data were used to calibrate and validate the hydrological model and to develop baseline climate and hydrologic balance components.

The other temporal data used for this study was RCMs rainfall and temperature simulation. Six RCMs (Table 1) which have showed good performance in capturing the historical (1981–2005) mean monthly and annual rainfall and frequency of rainfall events of the Jemma sub-basin (Worku et al., 2018b) were considered and acquired from the Coordinated Regional Climate Downscaling Experiment (CORDEX) Africa project. In each RCM, RCP8.5 which represents radiative forcing pathway of 8.5 W/m^2 by 2100, and RCP4.5 which represents intermediate emission levels of 4.5 W/m^2 that could start stabilization after 2100 (Moss et al., 2010) were used.

2.3. Bias correction of regional climate models simulation

The rainfall and temperature simulation of RCMs was further statistically bias corrected using robust bias correction method. The inter-comparison of different statistically bias correction method accentuates that all bias corrections methods have comparable performance in adjusting mean annual and monthly values. However, most bias correction methods struggle to bias correct the intensity and frequency of extreme values. Distribution mapping method was superior in adjusting the 90th percentile and wet day probability of RCMs simulation with observed counterparts (Worku et al., 2019). Different from other bias correction methods, distribution mapping method fits the distribution function (CDF) of RCM-simulated rainfall and temperature values with the CDF of corresponding observed values (Teutschbein and Seibert, 2012). Distribution mapping uses a shape parameter (α) and scale parameter (β) to fit distributions of rainfall (Fig. 3). These shape (α) and scale (β) parameters control RCMs daily rainfall probability of occurrences (distribution) and intensities, respectively (Gudmundsson et al., 2012; Teutschbein and Seibert, 2012). Thus, in this study, RCMs rainfall and temperature bias adjusted using distribution mapping method was used to run the hydrological model.

2.4. Hydrological model setup

The SWAT model is developed to predict the impact of land management practices on water, sediment and agricultural chemical yields in large complex watersheds with varying soils, land use and management conditions (Arnold et al., 1998). The model is successfully applied in Blue Nile Basin to study hydrological processes and other environmental applications (Setegn et al., 2011; Betrie et al., 2012; van Griensven et al., 2012). The SWAT model for the Jemma sub-basin was discretized into 150 sub-watersheds using a threshold area of 45 km^2. Within each of sub-watersheds, Hydrological Response Units (HRUs) were created. HRUs are unique combinations of slope, soil and land use. Multiple HRUs were defined in a sub-basin to allow heterogeneity within the basin. The slope was classified into 0–8%, 8–20% and > 20% to define the HRUs. The HRU definition processes created 958 HRUs. The Soil Conservation Service (SCS) Curve Number method (USDA-SCS, 1972) was used to estimate surface runoff. Potential evapotranspiration (PET) was estimated using the Penman–Monteith method since it is a physically based model.

2.5. Model calibration and validation

Before analysis of climate change impacts, the hydrological model was calibrated and validated to represent the hydrologic conditions of the sub-basin. The calibration of the model parameters was conducted using SUFI-2 in SWAT-CUP (Abbaspour et al., 2004). Since the SWAT model has hundreds of parameters, the most sensitive parameters which affect the simulation outputs were identified through sensitivity analysis. Parameters related to soil water, runoff, groundwater and evapotranspiration were considered for the sensitivity analysis. The highest sensitive parameters which have smaller p-value and larger t-stat were selected.

The Jemma sub-basin is large in area and it has diverse topography. Therefore, multi-gauge calibration and validation (Cao et al., 2006; Zhang et al., 2008; Santhi et al., 2009; Arnold et al., 2012b) approach was applied to capture the hydrological processes across the sub-basin. At Beressa and Robi-Gumero gauge stations which are located at the upper and middle part of the Jemma sub-basin (Fig. 1), streamflow data is available from 1991 to 2008 and 1988–2002 respectively. However, at the Jemma River gauging stations (outlet) of the Jemma sub-basin, streamflow data is available only from 1996 to 1997. Therefore, the model was calibrated at Beressa (2002–2008) using observed streamflow data of this gauging station. Semi-automatic calibration procedure was used to

Table 1
Description Regional Climate Models used in this study.

No.	RCMs	Driving GCM	Labels	RCM center/institute
1	CCLM	CNRM-CM5	CCLM4(CNRM-CM5)	Climate Limited-Area Modelling (CLM) Community
2	CCLM	EC-EARTH	CCLM4(EC-EARTH)	Climate Limited-Area Modelling (CLM) Community
3	CCLM	HadGEM2-ES	CCLM4(HadGEM2-ES)	Climate Limited-Area Modelling (CLM) Community
4	CCLM	MPI-ESM-LR	CCLM4(MPI-ESM-LR)	Climate Limited-Area Modelling (CLM) Community
5	REMO	EC-EARTH	CCLM4 (EC-EARTH)	Max Planck Institute (MPI),Germany
6	REMO	MPI-ESM-LR	CCLM4(MPI-ESM-LR)	Max Planck Institute (MPI),Germany

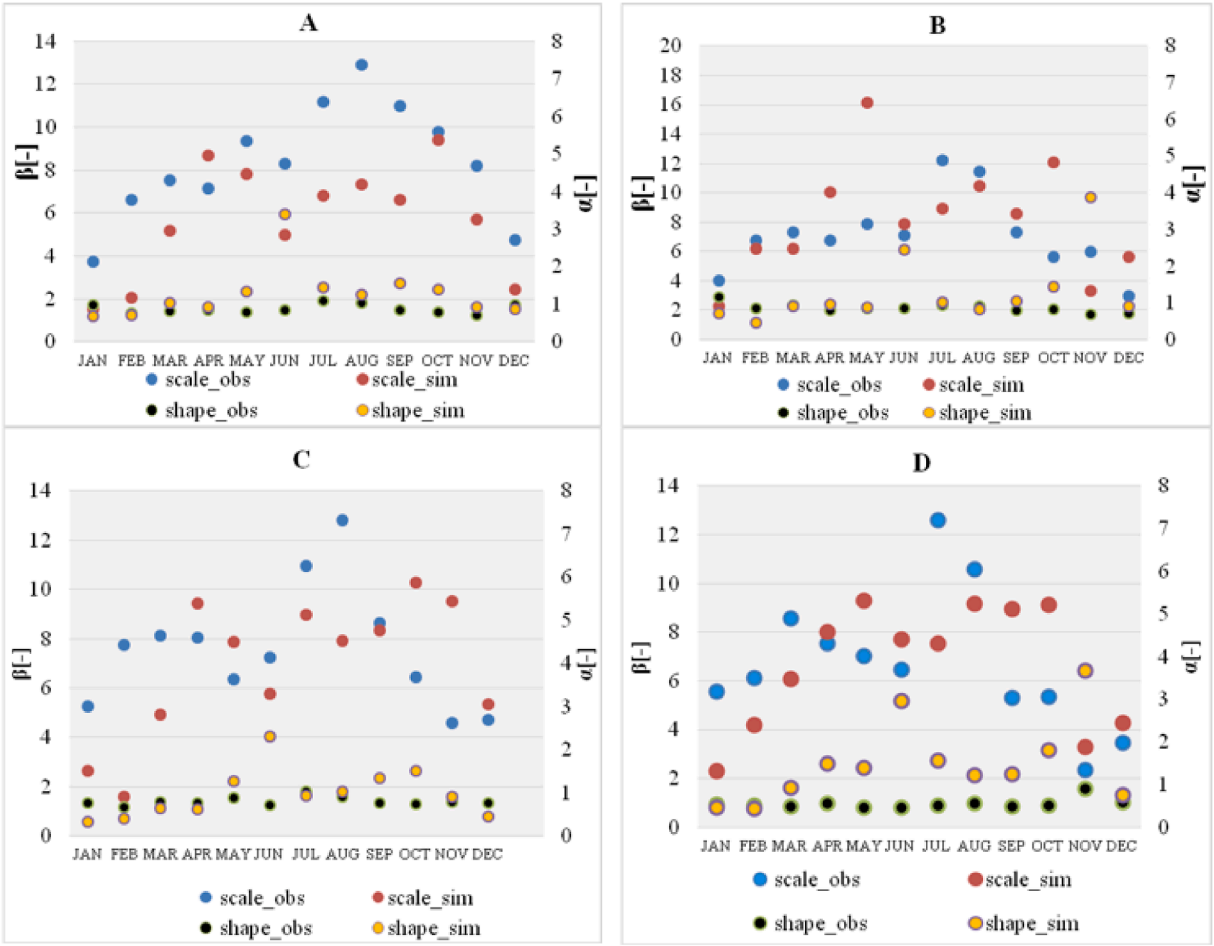

Fig. 3. Monthly scale parameters (β) and shape parameters (α) of the Gamma distribution fitting observed and raw RCM-simulated rainfall in Central (A), Eastern (B), Western (C) and North-eastern (D) areas of the Jemma sub-basin. Scale_obs, scale_sim, shape_obs and shape_sim are to indicate the scale and shape parameters of observed and RCMs simulated rainfall.

calibrate the model (Arnold et al., 2012b). The calibrated model was also validated at Beressa (1991–1999), Robi-Gumero (1991–2002) and Jemma (1996–1997) using observed streamflow of these gauge stations. Since the period from 1991 to 1995 was government transition period in Ethiopia, we assume the quality of data after 1995 is better and consequently used for calibration. Due to data scarcity, only validation was performed at Jemma gauge station. The observed streamflow data was representative for calibration and validation since it includes relatively high, moderate and low rainfall and streamflow years. For example, during calibration period of Beressa, low and high streamflow was observed in the year 2003 and 2007 respectively. Whereas, high and low streamflow was observed in 1994 and 1997 years of validation, respectively (Fig. 4).

The performance of the model during calibration and validation was evaluated using Nash and Sutcliffe simulation efficiency (NSE), percent Bias (PBIAS), RMSE-observations standard deviation ratio (RSR) and bR^2 which are important goodness-of-fit evaluation criteria (Moriasi et al., 2007, 2015; Abbaspour, 2015). The NSE is normalized statistics that measures the relative magnitude of the residual variance compared to the observed data variance (Nash and Sutcliffe, 1970). Generally, the NSE value ranges between 1 (when measured data and simulated are alike) and -∞. NSE > 0.50 is considered as an acceptable level of performance for streamflow simulation (Moriasi et al., 2015; Abbaspour, 2015). PBIAS measures the average tendency of the simulated data to be larger or smaller than the observed data. A PBIAS value ranges from -∞ to ∞ and an optimal value of PBIAS is 0 (Moriasi et al., 2015). A positive value of PBIAS indicates model underestimation and negative values indicates model overestimation. RSR measures the ratio of the Root Mean Square Error to the standard deviation of measured data. Its value ranges from 0 to large positive values. The lower the RSR considered as the better the model fit (Abbaspour, 2015). The bR^2 is a result of R^2 multiplied by the coefficient of the regression line, *b* between measured and simulated data (Abbaspour, 2015).

The uncertainty of model simulation was evaluated using P-factor and the r-factor on the SUFI-2 algorithm (Abbaspour et al, 2004; Abbaspour et al., 2007). The SUFI-2 estimates uncertainty at the 95 percent prediction uncertainty (95PPU). The P-factor is the percentage of the measured data bracketed within the 95PPU while the r-factor measures the thickness of the uncertainty band. P-factor of 1 and an r-factor of 0 indicates exact fit of simulation with measurement (Abbaspour et al., 2007; Abbaspour, 2015).

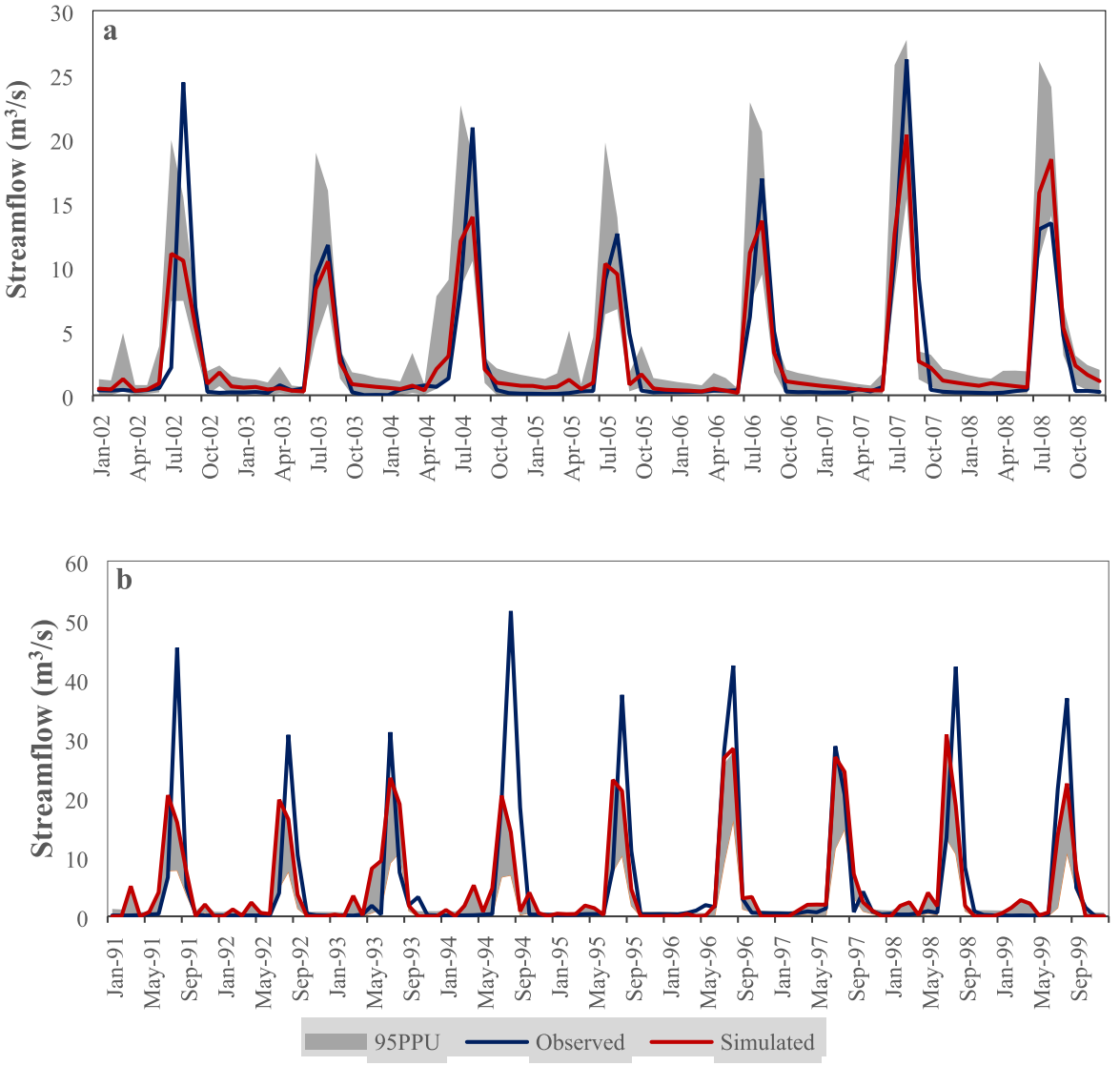

Fig. 4. Simulated and validated hydrographs of (a) calibration and (b) validation at Beressa gauge station of Jemma sub-basin.

2.6. Estimating hydrological climate change impact

To simulate hydrological impact of climate change, the ensemble mean of RCMs/GCMs is recommended (Teutschbein and Seibert, 2010; Taylor, et al, 2012). Thus, the ensemble mean of six statistically bias corrected RCMs rainfall and temperature output under RCP4.5 and RCP8.5 emission scenarios at each climatic station was used as input to hydrological model. The calibrated and validated SWAT model was used to estimate surface runoff, evapotranspiration and total water yield under baseline climate (1981–2013) and future climate scenarios. The impact on the hydrological variables was studied dividing the coming century into near-term (2021–2050) and long-term (2071–2100) future. The impacts of climate change were therefore analysed by comparing the ensemble mean of RCMs under RCP4.5 and RCP8.5 emission scenarios with the baseline climate (1981–2013). Besides to the ensemble mean of the RCMs, hydrological simulation was made using the input of the RCM (i.e CCLM4 (MPI-ESM-LR)) which was better in capturing the rainfall and temperature of the baseline period. As a result, CCLM4 (MPI-ESM-LR) model was used as input to the hydrological model and the output was compared with the hydrology simulated with ensemble mean output.

2.7. Analysis of trends of climatic variables and water balance components

To study trends of rainfall, TMAX, TMIN and water balance components, the non-parametric Mann-Kendal test (Kendall, 1975; Mann, 1945) was used. The trend result which is less than or equal to 5% was considered as statistically significant. The Mann-Kendall test statistic is calculated as;

$$Zs = \sum_{k=1}^{n-1}\sum_{j=k+1}^{n} \mathrm{sgn}\left(X_j - X_i\right) \tag{1}$$

$$sgn(x) = \begin{cases} 1 if x > 0 \\ 0 if x = 0 \\ -1 if x < 0 \end{cases} \tag{2}$$

Where X_j and X_j are the annual values in years j and i, j > i, respectively. A positive and negative value of Z*s* indicates an increasing and decreasing trend, respectively. Mann- Kendal test was selected because this test is non-parametric (distribution-free) and not sensitive to single outliers and skewed distributions. Therefore, for data of climatic variables and water balance components which are not normally distributed, it is commendable to use Mann-Kendall test for trend detection. The slope of trends of climatic variables and water balance components under different climate change scenarios was calculated using the non-parametric, Theil-Sen's slope estimator (Sen, 1968; Theil, 1950). The value of Sen's slope estimator indicates the steepness of the trend. It reflects the magnitude of the change in the variable at each year. Theil-Sen test estimates the median of the slopes (β) using the equation:

$$b_{Sen} = \mathrm{median}\left(\frac{y_j - y_i}{x_j - x_i}\right) \tag{3}$$

Where $i < j$ and $i = 1, 2, \ldots n$-1 and $j = 2, 3, \ldots, n$.

Both Mann-Kendal and Sen's slope estimator were estimated using the 'trend' package (Pohlert, 2016) which is built on R-statistical software (The R Core Team, 2015).

3. Result and discussion

3.1. Model calibration and uncertainty analysis

Using the global sensitivity analysis, sensitivity of twenty-six hydrological parameters for streamflow was tested. The Global sensitivity analysis showed that CN2 (Curve number), ESCO (Soil evaporation compensation factor), SOL_AWC (Available water capacity of the soil), OV_N (Manning's "n" value for overland flow) and CH_N2 (Manning's "n" value for the main channel) are the most sensitive parameters (Table 2). Most of the sensitive parameters are related to surface runoff and processes occurring at the soil and channel. However, groundwater related parameters; ALPHA_BF (Base-flow alpha factor) and GWQMN (Threshold water depth in the shallow aquifer required for return flow to occur) are also considered in the calibration based on the literature (Betrie et al., 2012; van Griensven et al., 2012) in the Upper Blue Nile Basin. The groundwater parameters are considered to maintain the hydrological mass balance since the surface and groundwater processes are intertwined. Unlike other studies in the Upper Blue Nile Basin, this study found OV_N as sensitive parameter to streamflow simulation. OV_N was useful to adjust the pattern of simulated monthly streamflow with the observed monthly streamflow.

The comparison between the observed and simulated monthly streamflow showed a very good model performance during calibration and validation periods. For example, the NSE, R^2, $bR^{2,}$ RSR and PBIAS values during the calibration of the model at the Beressa River gauge station were 0.78, 0.79, 0.60, 0.46 and −4.2% respectively (Table 3 and Fig. 4a). At Robi-Gumero gauge station, the NSE and PBIAS values during calibration was 0.76 and 2.3% respectively (Table 3 and Fig. 5a). Similarly during the validation, at Beressa gauge station, the model showed NSE of 0.59 and PBIAS of 9.4% which can be considered as acceptable model performance (Moriasi et al., 2015). Likewise, the model validation using observed monthly streamflow at the Robi-Gumero and Jemma River gauging

Table 2
Calibrated model parameters, parameter ranges, and final fitted values using observed monthly streamflow at the Beressa River gauge station of the Jemma sub-basin. The model was calibrated for the period 2002–2008.

Sensitive Parameters	Parameter description	Parameter ranges	Final Fitted values
r_CN2.mgt	Curve number	−0. 1–0.2	−0.057
v_ESCO.hru	Soil evaporation compensation factor	0.0–1.0	0.2175
r_SOL_AWC.sol	Available water capacity of the soil (mm)	−0.2–0.1	−0.040
r_OV_N.hru	Manning's "n" value for overland flow	−0.2–0.2	−0.179
v_CH_N2.rte	Manning's "n" value for the main channel	−0.0 1– 0.3	0.054
V_ALPHA_BF.gw	Base-flow alpha factor (days)	0.0–1.0	0.597
v_GWQMN.gw	Threshold water depth in the shallow aquifer required for return flow to occur (mm)	0.0–500	131.250

The qualifier (r_) refers to a relative change in the parameter where the default values are multiplied by 1 plus a factor in the parameter range, while (v_) refers to the substitution of the default parameter by a value from the parameter range. The extensions (e.g., .hru, .bsn, .gw, etc.) indicate the SWAT parameter family.

Table 3
Calibration and validation performance of the SWAT model at the Beressa, Robi Gumero and Jemma river gauging stations of Jemma sub-basin. Beressa, Ribit-Lemi and Jemma river gauging stations are located at the upper, middle, and downstream areas of the Jemma sub-basin.

Objective functions	River Stations			
	Beressa		Robi Gumero	Jemma
	Calibration (2002–2008)	Validation (1991–1999)	Validation (1991–2002)	Validation (1996–1997)
NSE	0.78	0.59	0.61	0.85
R^2	0.79	0.59	0.62	0.86
PBIAS	−4.2	9.4	−2.1	10.4
bR^2	0.60	0.32	0.42	0.70
RSR	0.46	0.64	0.62	0.39
P-factor (%)	80	71	68	64
R-factor	0.65	0.30	0.85	0.51

stations showed NSE of 0.64 and 0.85 respectively. PBIAS values of −5.0% and 10.4% were also found during validation at Robi-Gumero and Jemma River gauging stations respectively (Table 3, Fig. 5). The model also show acceptable performance of R^2, bR^2 and RSR during validation at different gauges.

The uncertainty analysis of the calibrated model provided very good P-factor and r-factor (P-factor > 70% and r-factor of close to 0) (Abbaspour, 2015). The calibrated model at Beressa River gauging station bracketed 80% and 71% of the observed data within the 95PPU during the calibration and validation periods, respectively. At Robi-Gumero and Jemma River gauging stations, P-factor of 68% and 64% respectively was also obtained. The measure of the uncertainty using the r-factor also showed performance of 0.65 during the calibration at the Beressa River gauging station. The validation of the model at the Beressa, Robi-Gumero and Jemma River gauging stations provided an r-factor of 0.3, 0.85 and 0.51, respectively. The best r-factor (i.e. smallest uncertainty band) was observed during the validation period at the Beressa and Jemma River gauging station (Table 3).

The calibrations and validations performed at different gauging stations showed very good performance in simulating the observed streamflow except the validation at Beressa River gauging station which could not capture the peak streamflow (Fig. 4b). This may be associated to poor quality of climate and/or streamflow data. The calibrated parameter sets at Beressa River gauging station simulates the streamflow of the Robi-Gumero and Jemma River gauging sites during validation. This suggests that the parameter sets are representative across the Jemma sub-basin. However, the model performance in terms of NSE was higher at the sub-basin outlet than at the watershed level (Table 3, Fig. 5b), which suggests that calibrating hydrological models only at the basin outlet may overrate performance of models than evaluating them at the watershed level. Similarly, Cao et al., (2006) and Begou et al., (2016), reported better performance of models at the watershed outlet than sub-watershed outlets at a large mountainous catchment of New Zealand and Bani Catchment of Niger River , respectively.

3.2. Hydrologic balance analysis under baseline climate scenario

The long-term mean annual water balance analysis of the sub-basin under baseline climate accentuates large proportion of the rainfall becomes evapotranspiration (51.68%) and surface run-off (40.32%) (Table 4). Jemma sub-basin has a total water yield (refers the sum of surface runoff, lateral flow and groundwater minus transmission losses) of 501 mm which is 48.21% of the total rainfall. In this sub-basin, surface runoff has high proportion (83.63%) to the total water yield. This is in contrast to the headwaters of the Upper Blue Nile Basin where, for example, Setegn et al. (2009) reported that in the Lake Tana sub-basin, groundwater flow contribution is higher than surface runoff contribution.

Water balance dynamics at dry (2002) and wet (1997) years and in different seasons (Table 4) of the study period was examined. Here, the term “dry” and “wet” is relative which represent years with lower and higher rainfall during the baseline climate. During these dry and wet years, surface runoff has showed large deviation than other components of hydrological balance. During the wet year (1996), there is high surface runoff and water yield and in this wet year, 90% of the water yield is generated from surface runoff (Table 4).

The hydrological system of the Jemma sub-basin is strongly responsive to rainfall occurrence and has high rainfall-runoff coefficient (45%) during the rainy season. Comparative estimates were also reported the rainfall to runoff conversion in different catchments of the Jemma sub-basin. For example (Hurni et al., 2005) reported 55% rainfall is converted into runoff in Andit-tid catchment of the Jemma sub-basin, whereas Gebrehiwot and Ilstedt (2011) reported that the rainfall-runoff coefficient at Beressa and Weizer catchment of the Jemma sub-basin is 57% and 80%, respectively. Thus, water resources management strategies which focus on surface runoff are to be designed for sustainable water resources development in the Jemma sub-basin. Because, surface runoff is the dominant hydrological component which is highly dependent on rainfall.

3.3. Bias correction of regional climate models simulation

Using distribution mapping bias correction method, the overestimation and underestimation of RCMs simulation of mean monthly rainfall was sufficiently attuned with observed mean monthly rainfall of the entire sub-basin (Fig. 6). The bias correction also adjusted the monthly rainfall distribution particularly the peak rainfall values. In the observation from 1981 to 2005, the highest observed

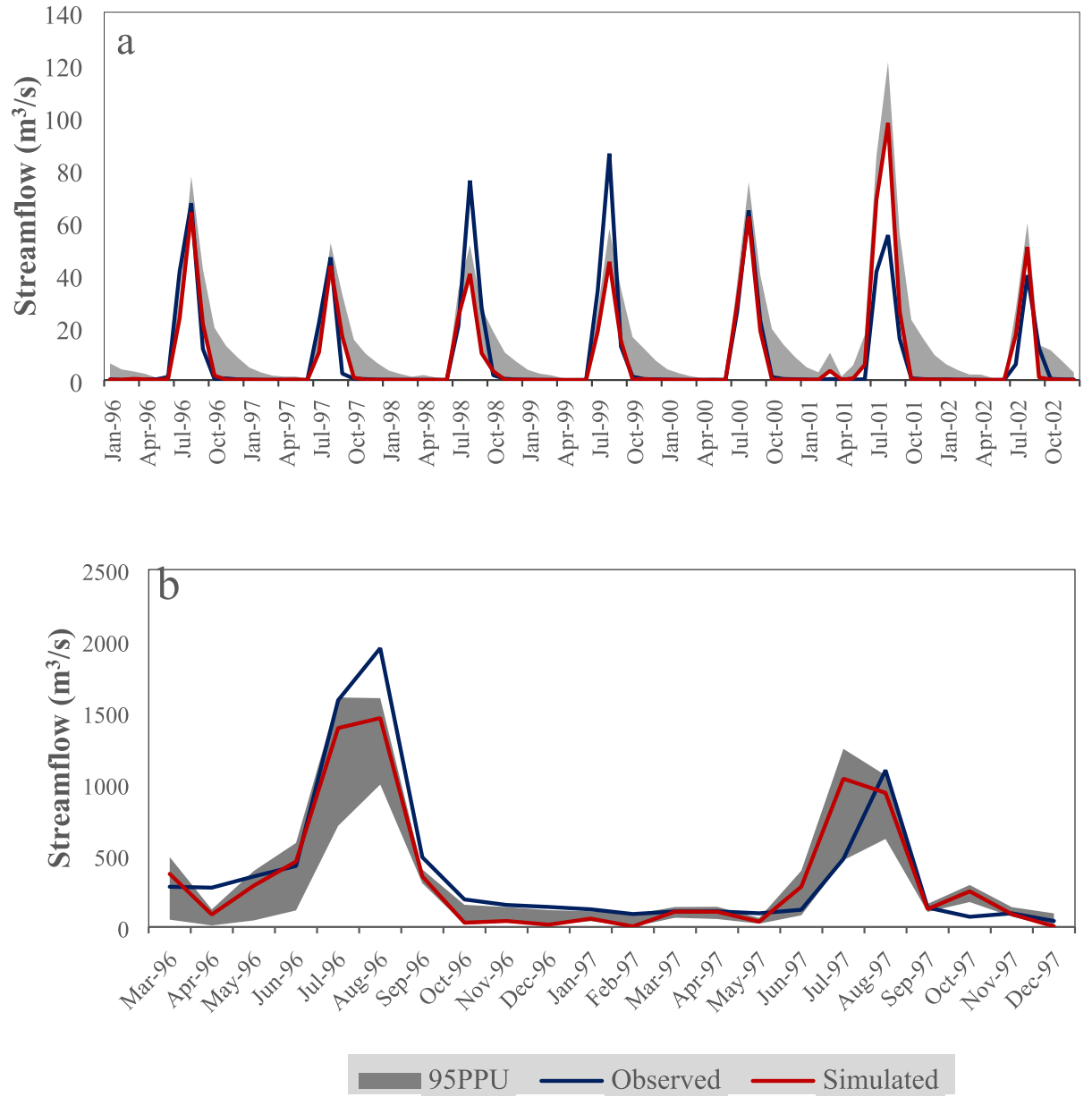

Fig. 5. Calibration and validation of SWAT model at Robi Gumero and Jemma gauge stations of the Jemma sub-basin. a) Calibration at Robi Gomero b) validation at Robi Gumero and c) validation at Jemma gauge station.

Table 4
Water balance components of the Jemma sub-basin in annual, dry and wet years. The estimates are based on the calibrated and validated model under baseline climate.

	Average (1981–2013)	Dry Year (2002)	Wet Year (1996)	Dry Season (Dec-Feb)	Rainy Season (Jun- Sep)
Rainfall (mm yr^{-1})	1039	801	1286	47.97	786.28
ET(mmyr^{-1})	537.30	510	645	50.00	282
SURQ(mm yr^{-1})	419.33	268	554	9.79	351
GWQ(mm yr^{-1})	67.81	27	77	3.43	41
LATQ(mm yr^{-1})	15.59	14	20	3.00	9.0
WYLD(mm yr^{-1})	500.84	303	642	16	390
PERC(mm yr^{-1})	86.12	27	81	0.72	57

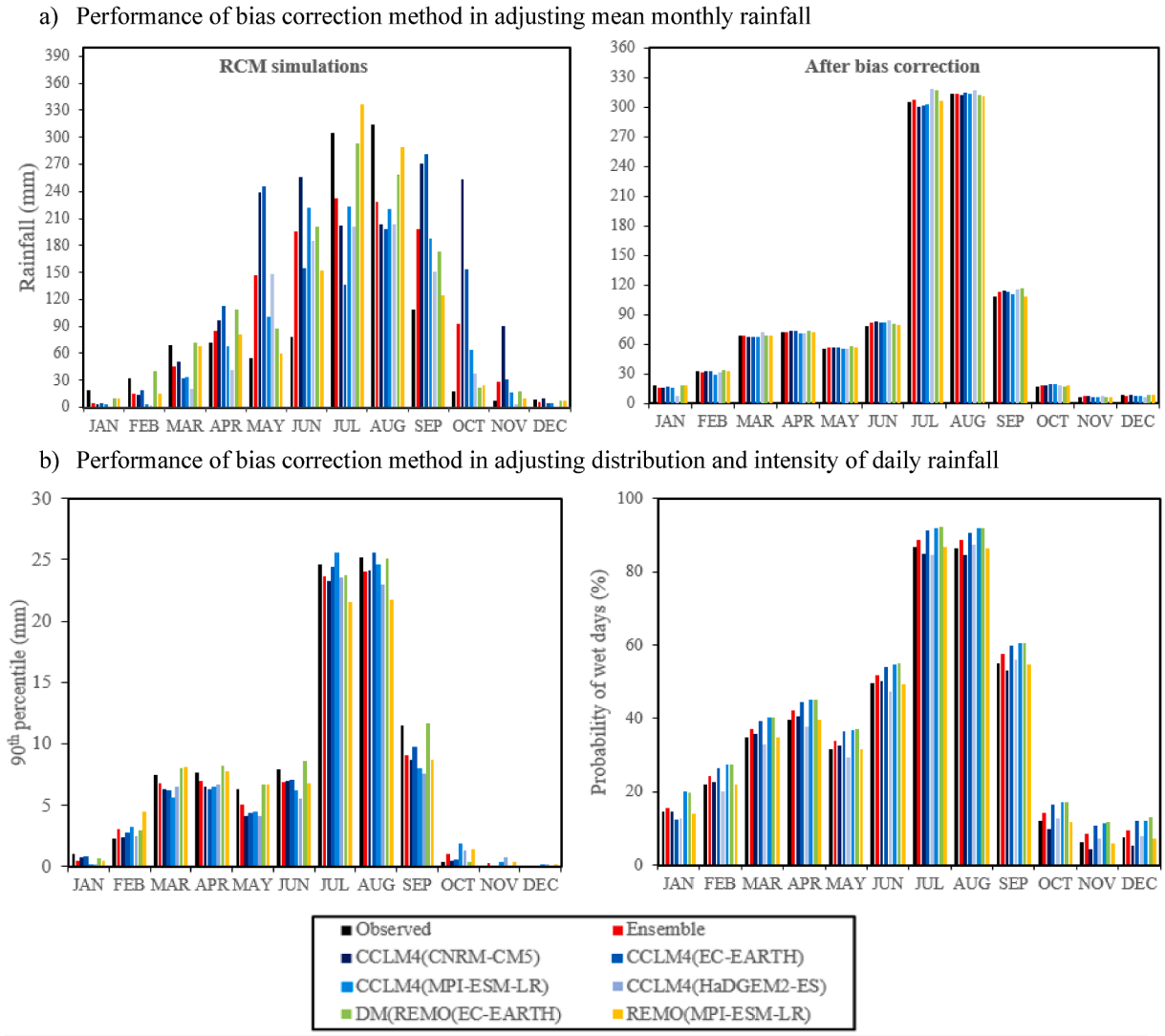

Fig. 6. Performance of bias correction method in adjusting mean, distribution and intensity of rainfall. a) Raw RCM simulations and RCM simulations after bias correction. b) Performance of bias correction technique in adjusting daily rainfall as measured by 90th percentile (mm) and probability of wet days (%). Values are area-weighted across the Jemma sub-basin.

monthly rainfall occurred in July and August, whereas some RCMs (CCLM (CNRM-CM5) and CCLM (EC-EARTH)) simulated higher rainfall occurred in September, October and May. In this regard, the bias correction effectively adjusts the RCMs simulation of mean monthly and seasonal rainfall biases. There are also other studies which have investigated that bias correction methods are able to correct climate models simulation (Elshamy et al., 2009; Teutschbein & Seibert, 2012; Fang et al., 2015; Bhatta et al., 2019).

RCMs simulation of TMAX and TMIN is characterized by steady overestimation and underestimation of TMIN and TMAX (Fig. 7). The overestimation of TMIN and underestimation TMAX by the RCMs was effectively adjusted with observed mean monthly TMAX and TMIN using bias correction (Fig. 7). Concomitantly, distribution mapping method was effective to adjust TMAX and TMIN simulation of GCMs at Addis Ababa of Ethiopia (Feyissa et al., 2018). Besides, different bias correction methods were also able to adjust mean daily, monthly and seasonal TMIN and TMAX of different RCMs simulation in Finchaa watershed of Blue Nile Basin (Geleta and Gobosho, 2018).

3.4. Rainfall and temperature under future climate scenarios

Future climate scenarios for the Jemma sub-basin were developed by blending different GCMs, RCMs, emission scenarios and robust bias correction method i.e distribution mapping. In the ensemble mean of RCM (E-RCMs), a consistent reduction of rainfall which ranges from 19% to 23% under all climate scenarios is detected. Large difference in rainfall change signal is observed among RCMs (S-RCMs) than among the ensemble mean of RCMs in the near and long-term climate scenarios. In the individual RCMs (S-

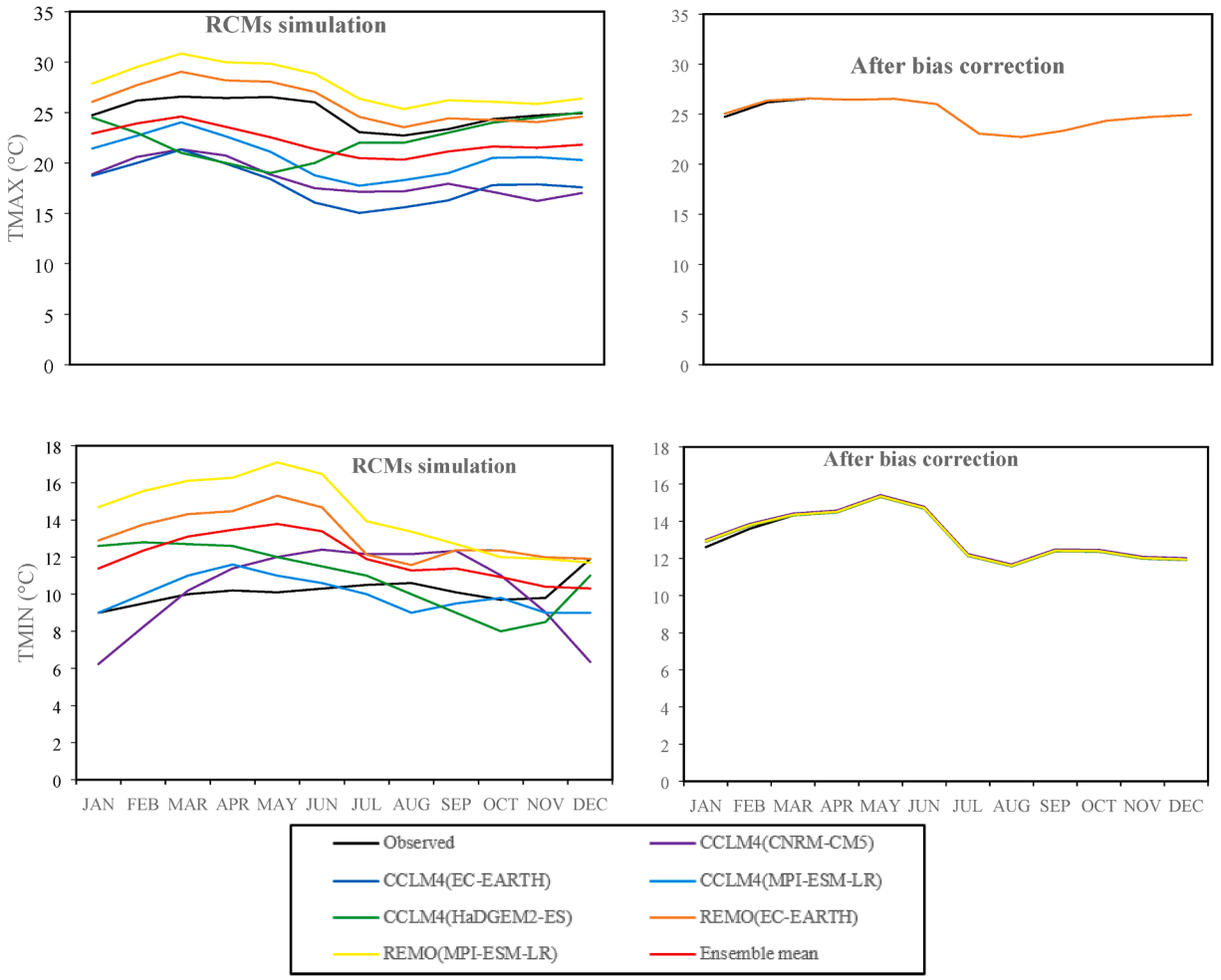

Fig 7. Mean monthly TMAX and TMIN (°C) of observed, RCMs simulation and statistically bias corrected RCMs outputs using distribution mapping. Values are area-weighted across the Jemma sub-basin.

RCMs), a subsidence of future rainfall is in the order of −43% to 0.5% for the near-term and from −42% to 12% for the long-term under RCP8.5 scenario. Whereas unpredictable response of rainfall to emission scenarios is projected. Higher reduction of rainfall is projected in the near-term than long-term climate condition under RCP8.5 emission scenario (Fig. 8). In the RCP4.5 emission scenario, higher reduction of rainfall is projected in the long-term climate condition than the near-term climate condition.

Seasonally, all seasons showed a reduction of rainfall except autumn season in which persistent increase of rainfall in future climate scenarios is projected (Table 5). High volumetric reduction of rainfall is projected in summer season, but high percentage reduction of rainfall is estimated in spring (March-May) followed by winter (December–February) seasons than summer under future climate scenarios. Positive change on autumn rainfall indicates there will be slight shifts of seasonal rainfall from summer to autumn. Concomitantly, multi-model ensemble mean project a shift in seasonal patterns of rainfall, with decreasing and increasing of rainfall in the June to July and August to November respectively in the Upper Blue Nile Basin (Liersch et al., 2016). In contrast to change on the dry season (spring and winter), Worqlul et al. (2018) has investigated an increase of dry season rainfall in future climate in Upper Blue Nile Basin using the downscaled outputs of HadCM3 climate model.

All individual RCM outputs showed a decrease in mean monthly rainfall in the near-term and long-term future except GCMs downscaled using REMO model (Fig. 9). Consequently, the ensemble mean monthly rainfall under all climate scenarios showed a decrease under both RCP scenarios. Concurrently, ensemble of different RCMs have projected a decrease of rainfall during the 2060 s and 2080 s periods under RCP4.5 and RCP8.5 scenarios in the Himalayan River Basin (Bhatta et al., 2019). Besides, the ensemble mean of multiple models also project a decrease of rainfall during the mid (2040–2069) and late (2070–2099) century under A2 and B1 emission scenarios in the Nile River Basin (Beyene et al., 2010).

In all climate scenarios, an increase of TMAX and TMIN is projected in the RCMs and in the ensemble mean of RCMs. In the ensemble mean of RCMs, a consistent increase of TMAX which ranges from1.01 °C to 3.13 °C is detected under future climate scenarios. Similarly, a consistent increase of TMIN which ranges from 1.14 °C to 5 °C is projected under future climate scenarios. In contrast to the projected rainfall, large difference in projected TMAX and TMIN is detected among emission scenarios than among

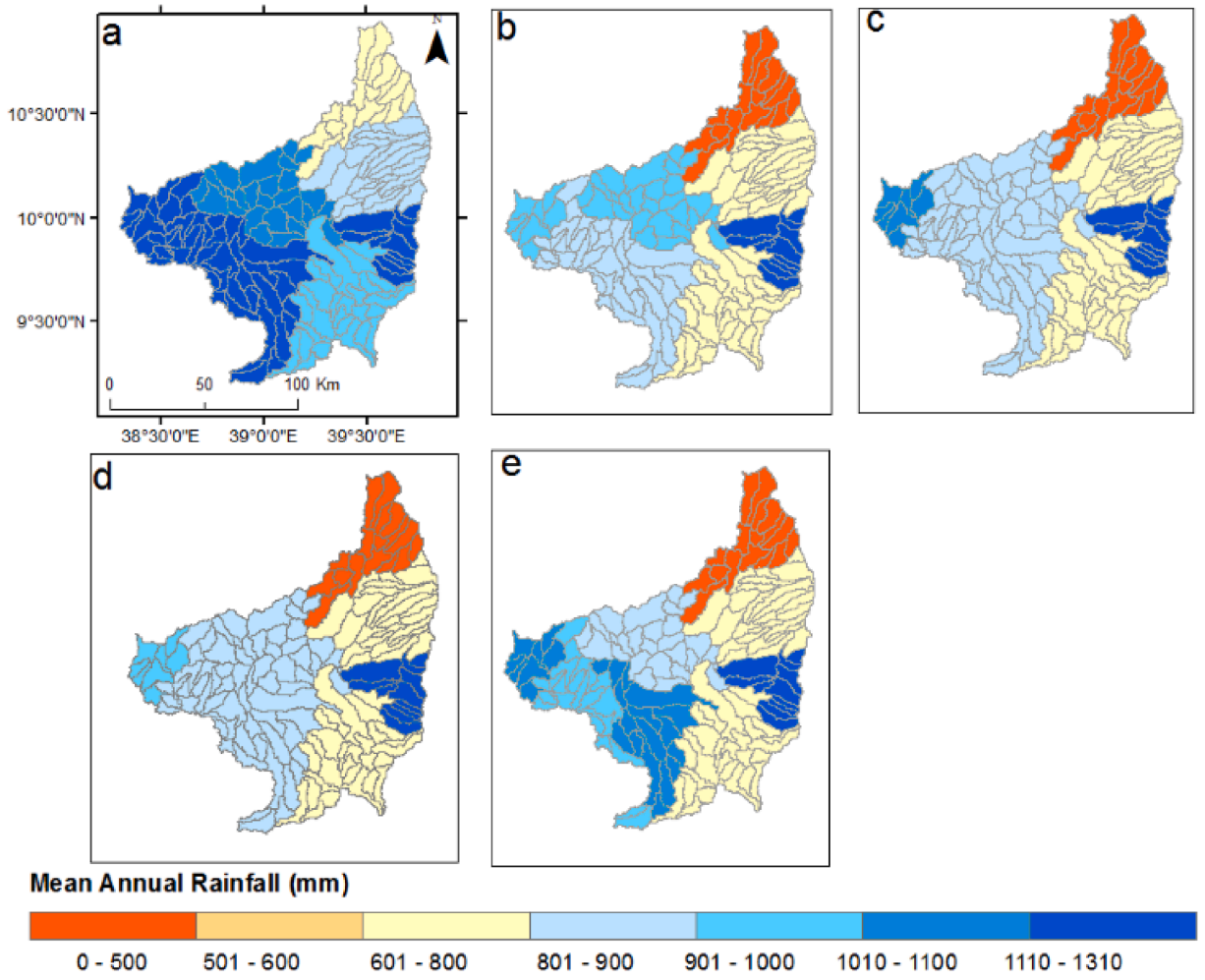

Fig. 8. Mean annual rainfall (mm) in baseline and future climate scenarios in each sub-watershed of the Jemma sub-basin; a) baseline climate, b) ensemble mean (2021–2050) RCP4.5, c) ensemble mean (2021–2050) RCP8.5, d) ensemble mean (2071–2100) RCP4.5 and e) ensemble mean (2071–2100) RCP8.5.

Table 5
Mean seasonal rainfall (mm) under baseline and future climate scenarios. The changes in the water balance components were estimated for an ensemble mean of RCMs under RCP4.5 and RCP8.5 emission scenarios.

Rainfall (mm yr^{-1})	Baseline (1981–2013)	Near-term 2021–2050 (RCP4.5)	Near-term 2021–2050 (RCP8.5)	Long-term 2071–2100 (RCP4.5)	Long-term 2071–2100 (RCP8.5)
Summer (June - September)	786	637(-19%)	628(-20%)	626(-20.35%)	673(-14%)
Spring (March - May)	168	118(-30%)	108(-36%)	101(-40%)	90(-46%)
Winter(December - February)	48	20(-58%)	17(-65%)	16(-67%)	19(-60%)
Autumn (October - November)	36	39(8%)	41(14%)	45(25%)	49(36%)

RCMs. Higher increase of TMIN and TMAX is estimated from climate scenarios under RCP8.5 emission scenarios. The Fifth IPCC assessment report has also attributed that emission scenarios are major drivers of temperature change (IPCC, 2013). Again in agreement with the projected concentration of greenhouses gases, high increase of TMAX and TMIN is projected in the long-term future than the near-term future. The individual RCMs and the ensemble mean of RCMs project higher increase of TMIN than TMAX under near and long-term climate scenarios. In general, TMAX and TMIN under all climate scenarios have shown strong agreement with the projected global temperature. This substantiates there will be high increase of temperature unless substantial and sustainable measures are to limit greenhouse gases emission by the global society are realized.

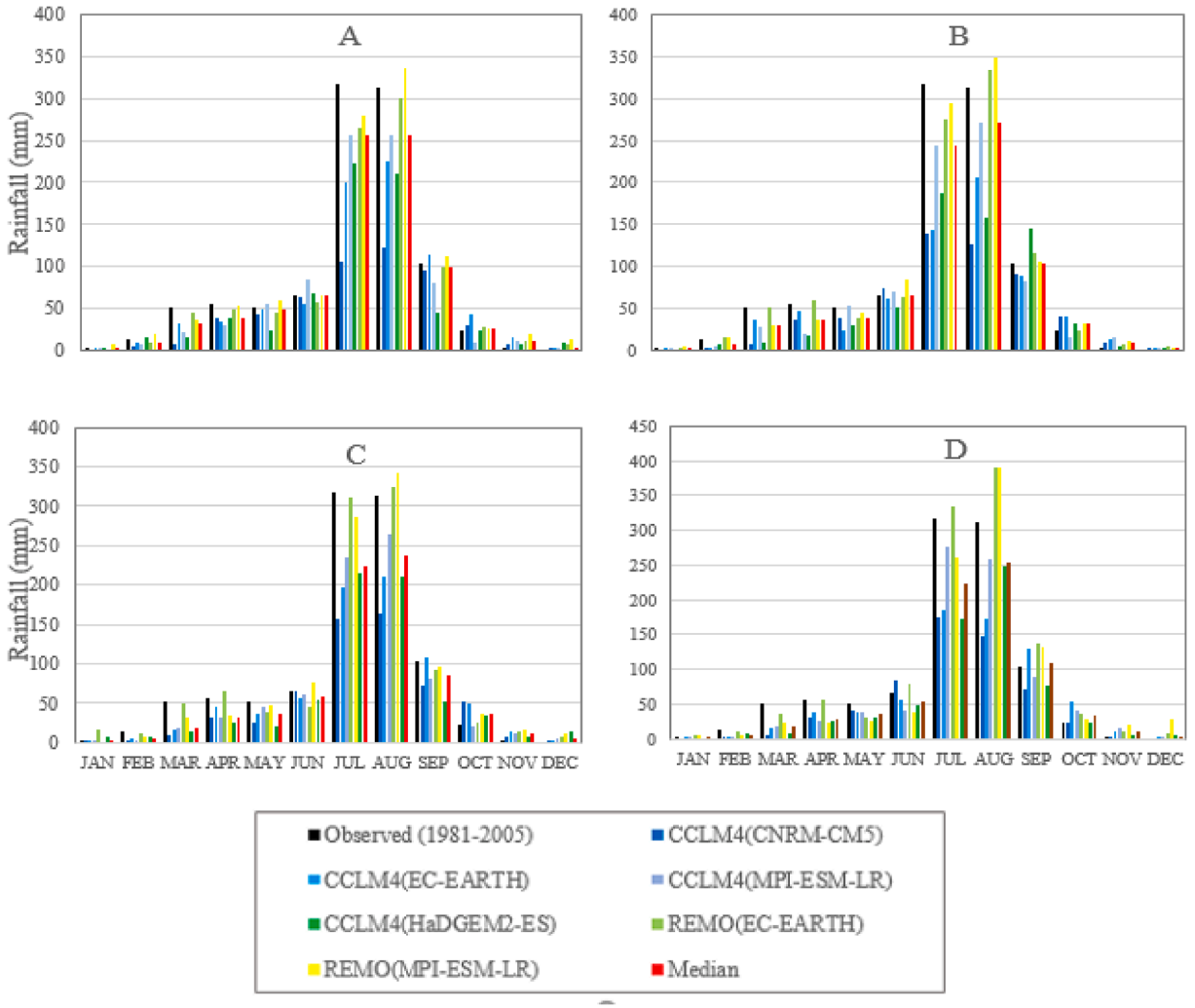

Fig. 9. Mean monthly rainfall under future climate scenarios. A) near-term (2021–2050) RCP4.5, B) near-term (2021–2050) RCP8.5, C) long-term (2071–2100) RCP4.5 and D) long-term (2071–2100) RCP8.5. The scenarios were done using the RCPs (Representative Concentration Pathways) 4.5 and 8.5. Values are area-weighted across the Jemma sub-basin.

3.5. Trends of rainfall and temperature under baseline and climate scenarios

Rainfall, TMAX and TMIN under different climate change scenarios exhibited different trends. Rainfall under baseline climate scenario showed an increasing but insignificant trend. However, the rainfall in the near-term climate scenarios revealed a negative trend. Even statistically significant negative change is detected in the rainfall under RCP8.5 (2021–2050) climate scenario (Table 6 and Fig. 10). Despite negative change from the baseline rainfall, the trend of rainfall under the long-term climate scenarios is positive. This

Table 6
Trend of Rainfall, TMAX and TMIN under baseline and future climate scenarios in the Jemma sub-basin.

Stations	Rainfall		TMAX		TMIN	
	Zs	b_{sen}	Zs	b_{sen}	Zs	b_{sen}
Baseline (1983–2013)	1.22	2.4	0.05 *	3.90	0.05 *	3.90
RCP4.5 (2021–2050)	*−0.49*	−1.16	4.67**	0.03	5.67**	0.08
RCP8.5 (2021–2050)	*−2.34***	−10.99	4.64**	0.05	5.31**	0.10
RCP4.5 (2071–2100)	0.68	0.45	1.89	0.01	1.50	0.01
RCP8.5 (2071–2100)	0.21	0.59	5.56**	0.06	6.20**	0.10

Zs and b_{sen} are Mann-Kendal test and Sen Slope values respectively.
*Statistically significant trends at the 5% significance level.
**Statistically significant trends at the 1% significance level.

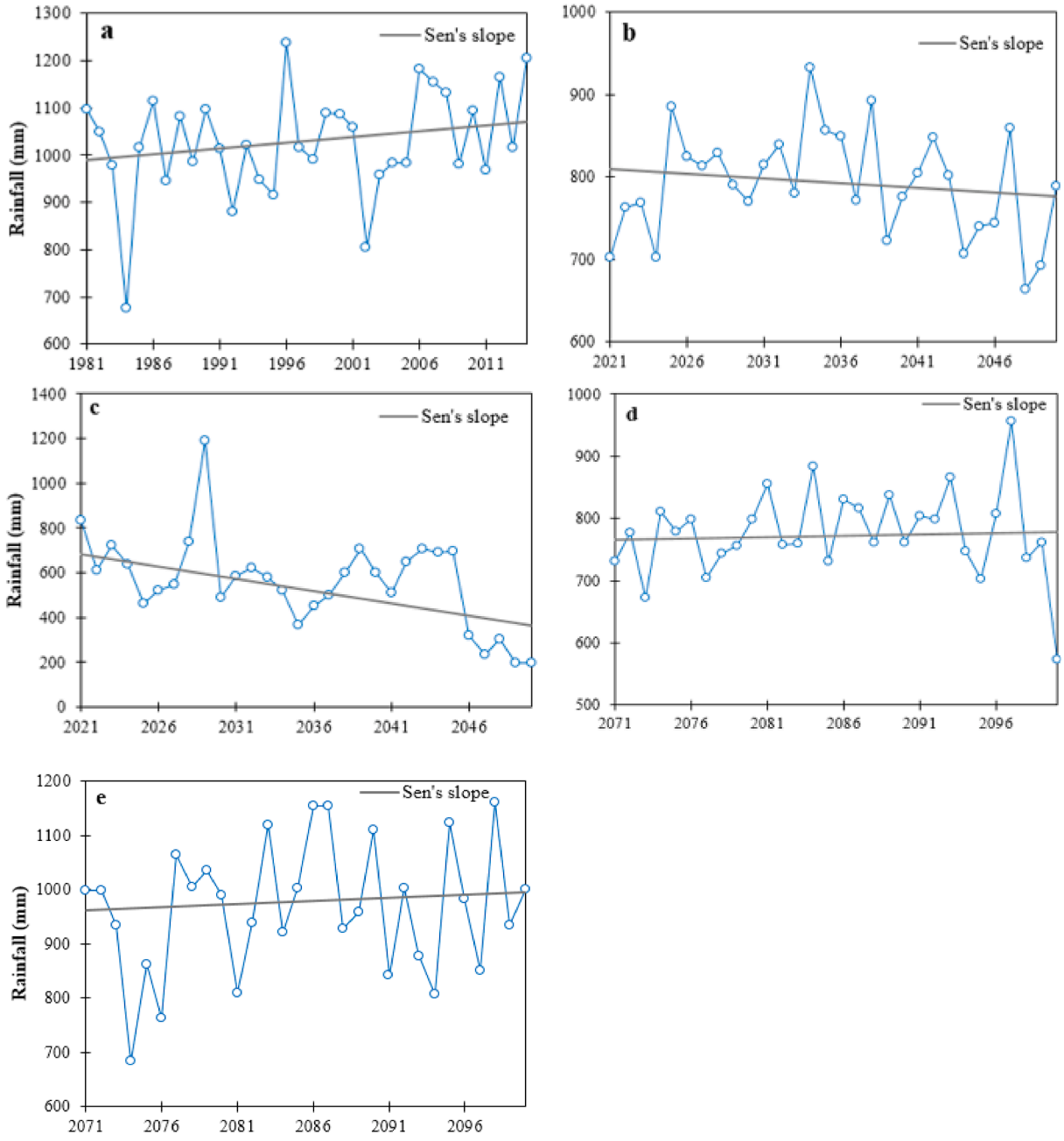

Fig. 10. - Trend of annual rainfall under baseline and different future climate change scenarios. a) Baseline climate scenarios, b) near-term (2021–2050) ensemble mean of RCP4.5, c) near-term (2021–2050) ensemble mean of RCP8.5, d) long-term (2071–2100) ensemble mean of RCP4.5 and e) long-term (2071–2100) ensemble mean of RCP8.5.

indicates there is an increase in rainfall within the climate window of 2071 – 2100.

Concomitant to global trend and consecutive IPCC reports, TMAX and TMIN showed statistically significant increase but differ in magnitude under baseline and future climate scenarios (Table 6). In most climate scenarios, the trend in TMAX and TMIN is statistically significant (at 1% and 5% level). It is only in the RCP4.5 (2071–2100) climate scenario the trend is not significant. This is simultaneous with the mean change in TMAX and TMIN which show a positive deviation from TMAX and TMIN of the baseline climate. In most of the climate scenarios, the trend in TMIN is higher than TMAX. The mean of future climate scenarios also show higher increase in TMIN than TMAX from the baseline climate. The trends in TMAX and TMIN under different climate scenarios suggest that climate change is behind the increase in temperature in the Jemma sub-basin. This study also investigated great similarity between the

results of Mann-Kendall and Sen's slope statistical tests.

3.6. Water balance components under different future climate scenarios

The change in rainfall and temperature due to the future climate was seen to trigger a change on the water balance components in the Jemma sub-basin. Although there is a difference in magnitude, the surface runoff showed a decline under all the future climate scenarios. The highest reduction of surface runoff (-65%) was observed in the near-term period (2021–2050) and under RCP8.5 climate scenario. Over long-term climate scenario (2071–2100), the reduction in surface runoff was smaller both in the RCP4.5 and RCP8.5 emission scenarios (Table 7 and Fig. 11). This may be attributed to the better rainfall in the long-term climate scenarios compared to the near-term climate scenarios. Generally, the reduction in surface runoff is related to the reduction in rainfall. The highest reduction in surface runoff occurred during the main rainy season (June-September) (Fig. 14). Spatially, in the sub-watersheds located in the northern and southern areas, there will be higher reduction of surface runoff under the near term and long-term climate scenarios (Fig. 11).

For the coming century, annual rainfall and surface runoff may decrease, however evapotranspiration may increase. The increase in actual evapotranspiration is in partly due to a consistent increase in temperature. Similar to the surface runoff, there will be lower actual evapotranspiration in the northern part of the sub-watersheds under all future climate scenarios (Fig. 12). Lower soil water and rainfall in the northern part of the sub-watersheds could result low actual evapotranspiration since it is changed due to changes in temperature and soil water (Olsson et al., 2016).

The total water yield may decrease for the coming century due to the impact of future climate change. The magnitude and spatial pattern of change was similar to the impact to surface runoff (Table 7). The largest reduction of water yield (-56%) was estimated from the near-term ensemble mean of RCP8.5 and long-term RCP4.5 scenarios, where the highest reduction of rainfall and surface runoff was projected (Table 7). Higher water yield is projected in the long-term ensemble of RCP8.5 than other future climate scenarios primarily due to the higher projected rainfall and surface runoff in this climate scenario. The reduction of total water yield may cause rampant impacts on the agriculture, domestic and livestock water supply and other ecosystem services in the Jemma sub-basin. The northern and the southern sub-watersheds will be characterized by lower water yield than other areas of the basin (Fig. 13). These areas of the sub-basin are also characterized by low water yield under the baseline climate scenario and in these areas, low surface runoff is projected.

Groundwater is another water balance component which will be affected by anticipated climate change. In this study, there will be higher drop of groundwater under climate scenario of RCP4.5 (2071–2100) (Fig. 14). This could be due to high loss of water through evapotranspiration in this climate scenario in which an increase and higher evapotranspiration is projected than other climate scenarios. Different from surface runoff and total water yield, there is no sharp decline of groundwater in the months of September to November, the maximum groundwater flow is during September (Fig. 14d). The monthly hydrography of the groundwater flow also indicates there is one-month lag-time between surface runoff and groundwater flow (Fig. 14).

Seasonally, a reduction of surface runoff, groundwater discharge and water yield are estimated in all seasons under future climate scenarios. However, the magnitude of change is different among seasons. High volumetric reduction of surface runoff and water yield is estimated in summer season, while high percentage reduction of surface runoff, water yield and groundwater discharge is estimated in spring (March-May) followed by winter (December–February) seasons than summer season under future climate scenarios (Table 8). This indicates dry seasons will be more water constrained in the future climate condition. Even though, persistent increase in autumn season rainfall is projected under future climate scenarios, this season is among the seasons showed higher subsidence of water availability. This could be due to the increase in temperature which trigger loss of water through evapotranspiration.

In contrast to surface runoff, groundwater and water yield, future climate will be characterized by an increase and more loss of water through evapotranspiration during different seasons. This might be attributed to an increase in temperature in the future climate scenarios. This corroborates that the increase in evapotranspiration alone could trigger the sub-basin become more water constrained, which is the case for Blue Nile Basin (Elshamy et al., 2009). Lower loss of water through evapotranspiration is estimated in spring and

Table 7
Mean annual water balance components under baseline climate future climate scenarios. The changes in the water balance components were estimated for an ensemble mean of RCMs under RCP4.5 and RCP8.5 emission scenarios.

	Baseline (1981–2013)	Near-term 2021–2050 (RCP4.5)	Near-term 2021–2050 (RCP8.5)	Long-term 2071–2100 (RCP4.5)	Long-term 2071–2100 (RCP8.5)
Rainfall (mm yr^{-1})	1039	799 (-20%)	782(–22%)	791 (-21%)	812(-19%)
ET(mm yr^{-1})	537.30	584.39(9%)	574.60(7%)	565.40 (5%)	557.29(4%)
SURQ (mm yr^{-1})	419.33	191.46(-57%)	185.27(-58%)	190.41(-57%)	226.07(-48%)
GWQ (mm yr^{-1})	67.81	37.61(-44%)	36.20(-47%)	32.17(-52%)	40.41(-40%)
LATQ(mm yr^{-1})	15.59	11.99(–23%)	8.73(-44%)	10.95(-29%)	8.62(-45%)
WYLD (mmyr^{-1})	500.84	231.02(-54%)	220.02(-56%)	222.19(-56%)	266.03(-47%)
PERC(mmyr^{-1})	86.12	47.77(-44%)	45.90(-47%)	40.83(-53%)	51.28(-40%)

ET = evapotranspiration, SURQ = surface runoff, GWQ = groundwater contribution to streamflow, LATQ = lateral flow into stream, WYLD (total water yield) = SURQ + LATQ + GWQ-LOSSES, PERC = percolation below root zone (groundwater recharge).

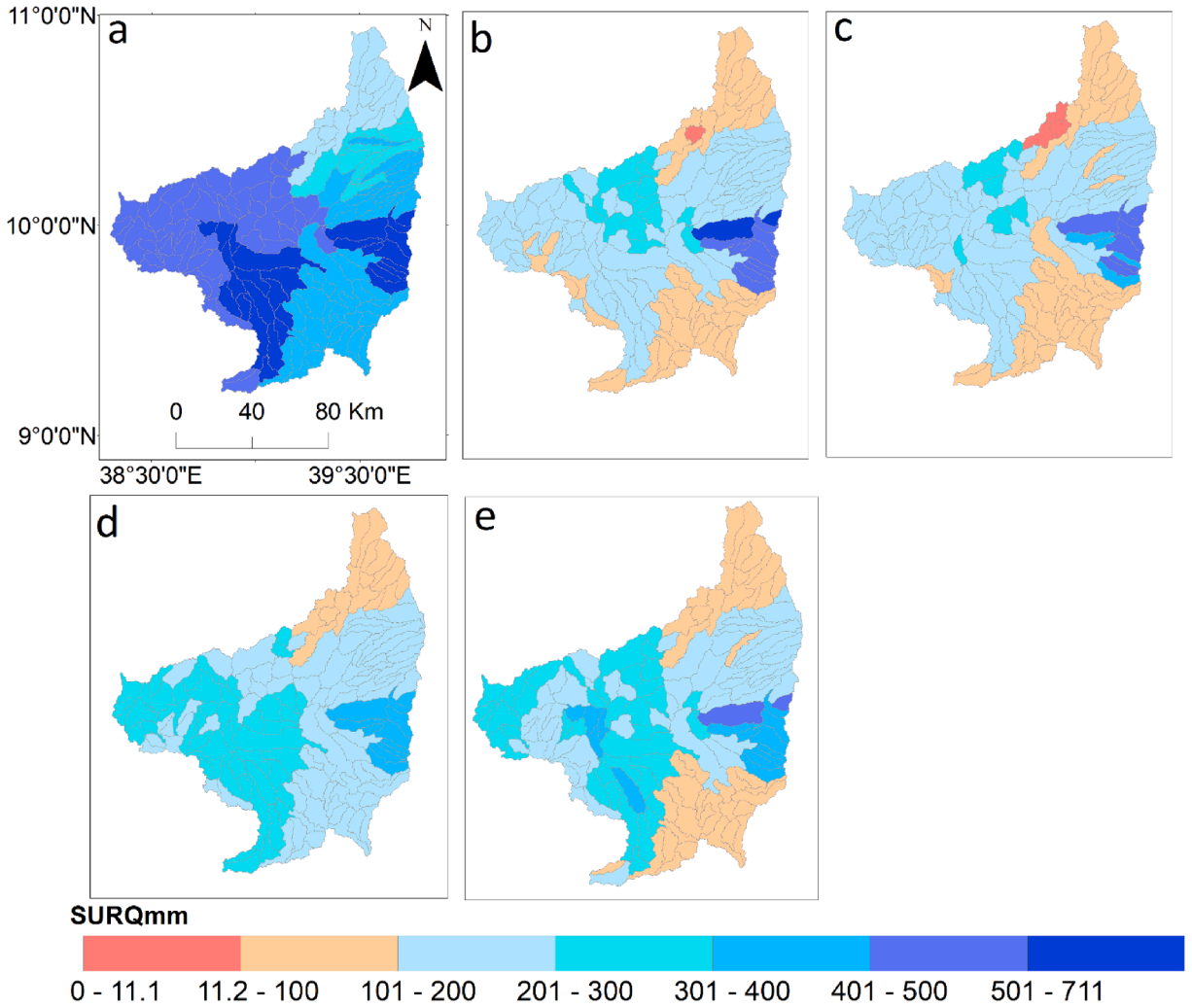

Fig. 11. Mean annual surface runoff (SURQmm) under baseline and future climate scenarios in each sub-watershed of the Jemma sub-basin. a) baseline (1981–2014), b) near-term (2021–2050) ensemble mean of RCP4.5, c) near-term (2021–2050) ensemble mean of RCP8.5, d) long-term (2071–2100) ensemble mean of RCP4.5 and e) long-term (2071–2100) ensemble mean of RCP8.5 climate scenarios.

winter seasons under future climate scenarios than the baseline scenario. This might be due to the reduction of water available for evapotranspiration in spring and winter seasons in the future climate scenarios (Table 8).

The effect of climate change on water balance components was also investigated using the bias corrected output of CCLM4 (MPI-ESM-LR), which has showed better performance in capturing the rainfall and temperature of the historical (1981–2005) period. A concomitant change on water balance components is estimated using the output of CCLM4 (MPI-ESM-LR) and ensemble mean of RCMs. However, lower subsidence of surface runoff, water yield and groundwater flow are estimated using CCLM4 (MPI-ESM-LR) model than the ensemble mean of RCMs. For instance, a decrease of surface runoff by 47%, 51%, 54% and 53% is estimated using CCLM4(MPI-ESM-LR) model under, 2021–2050 (RCP4.5), 2021–2050 (RCP8.5), 2071–2100 (RCP4.5) and 2071–2100 (RCP8.5) climate scenarios respectively (Table 9). Correspondingly, a decrease of surface runoff by 57%, 58%, 57% and 48% is projected using the ensemble mean of RCMs under, 2021–2050 (RCP4.5), 2021–2050 (RCP8.5), 2071–2100 (RCP4.5) and 2071–2100 (RCP8.5) climate scenarios respectively (Table 7). In general, comparable signal of change on rainfall, surface runoff evapotranspiration, total water yield and groundwater is estimated using the output of ensemble mean of RCMs and CCLM4 (MPI-ESM-LR) model.

In the Upper Blue Nile Basin, there are different studies which project the negative and positive impact of climate change on the water resource base of the basin. For instance, in Tana sub-basin of Upper Blue Nile Basin, a reduction in surface runoff and an increase in evapotranspiration is also projected using the output of 15 GCMs and SWAT hydrologic model (Setegn et al., 2011). Worqlul et al., 2018 also project a reduction of average streamflow and an increase of evapotranspiration in the Beles basin of the Upper Blue Nile Basin. Conversely, an increment of streamflow is projected using the output of single GCM (HadCM3) and SWAT hydrological model in the Upper Gilgel Abay Catchment of Blue Nile Basin (Adem et al., 2016). Even with and without a change on rainfall, an increase in temperature and potential evapotranspiration lead reduced wet season runoff and the Upper Blue Nile Basin may become more

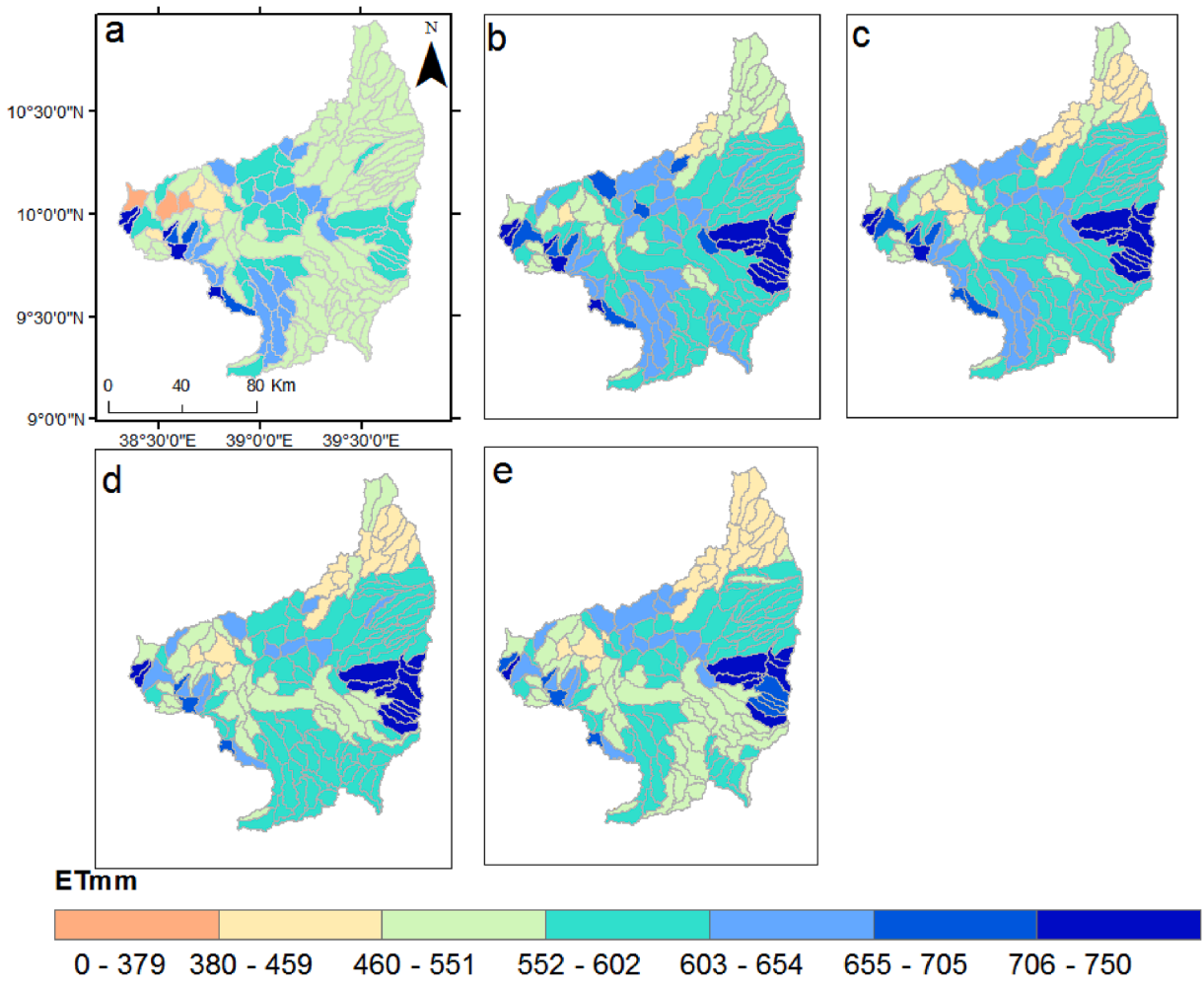

Fig. 12. Mean annual actual evapotranspiration (ETmm) under baseline and future climate scenarios in each sub-watershed of the Jemma sub-basin. a) baseline (1981–2013), b) near-term (2021–2050) ensemble mean of RCP4.5, c) near-term (2021–2050) ensemble mean of RCP8.5, d) long-term (2071–2100) ensemble mean of RCP4.5, and e) long-term (2071–2100) ensemble mean of RCP8.5.

moisture constrained in the future (Elshamy et al., 2009). In Jemma sub-basin and other studies particular to Upper Blue Nile Basin (Elshamy et al., 2009; Setegn et al., 2011; Liersch et al., 2016; Worqlul et al., 2018), a consistent increase in temperature is projected and this would intensify a decline in water availability through evapotranspiration.

3.7. Trends of hydrologic components under baseline and future climate scenarios

Similar with climatic variables, trend of water balance components under different climate scenarios was analyzed. Parallel to an increasing trend of rainfall and temperature under the baseline climate scenario, surface runoff, total water yield, groundwater and actual evapotranspiration revealed a positive trend (Table 10). While surface runoff, total water yield and groundwater showed consistent decreasing trend under most of future climate scenarios (Table 10). Particularly, statistically significant reduction of surface runoff is detected under RCP8.5 (2021–2050) and RCP4.5 (2071–2100) climate scenarios. In contrast actual evapotranspiration showed consistent increase under baseline and future climate scenarios. Even the change in actual evapotranspiration is statistically significant (at 5% level) under RCP8.5 (2021–2050) and RCP8.5 (2071–2100) climate scenarios. Such trend on water balance components and climatic variables could trigger compound effects which heighten effect of climate change in the sub-basin.

3.8. Uncertainties

The observed rainfall and temperature is captured by the raw simulation of RCMs and it is within the uncertainty range of rainfall and temperature simulated by different RCMs (Fig. 6a and Fig. 7). The ensemble mean is within the uncertainty range of different RCMs simulation and capture the seasonal pattern of the mean monthly observed rainfall, TMAX and TMIN. Particularly, the ensemble

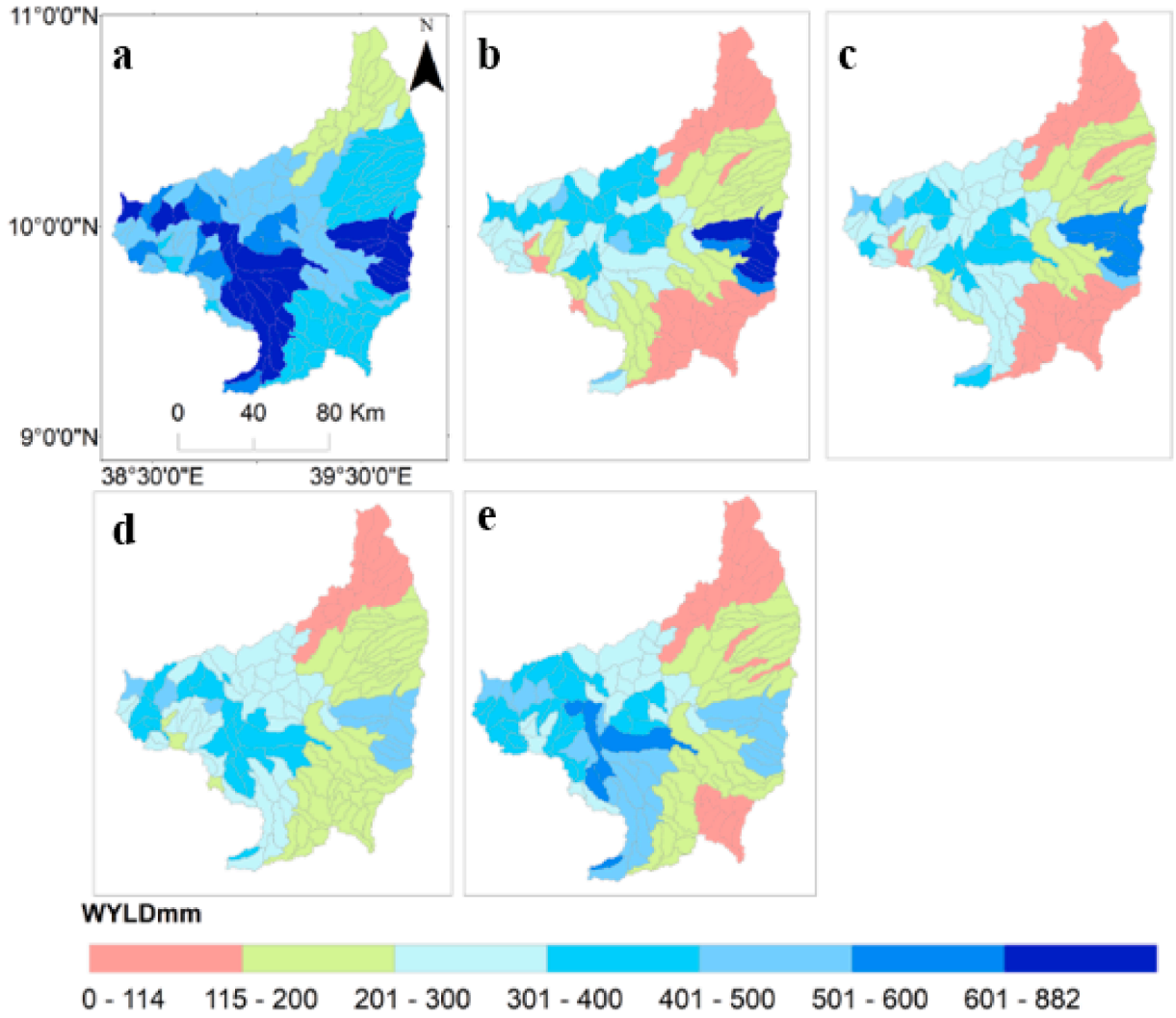

Fig. 13. Mean annual water yield (WYLDmm) under baseline and future climate scenarios in each sub-watershed of the Jemma sub-basin. a) Simulated water yield for the a) period 1981–2013, b) near-term (2021–2050) ensemble mean of RCP4.5, c) near-term (2021–2050) ensemble mean of RCP8.5, d) long-term (2071–2100) ensemble mean of RCP4.5 and e) long-term (2071–2100) ensemble mean of RCP8.5 climate scenarios.

mean is superior in capturing the observed mean monthly TMAX than other S-RCM. The uncertainties between the RCMs simulation and observation were adequately adjusted through bias correction (Fig. 6 and Fig. 7). Therefore, this was germane to use the ensemble of bias adjusted RCMs output to input hydrological model. The RCM i.e CCLM4 (MPI-ESM-LR) simulation which showed better performance in capturing the historical climate of the basin was also used to fed the hydrological model. Most of the RCMs and the ensemble mean showed uniformity in climate change signal, but with different magnitude. The GCMs downscaled through REMO model project lower reduction of rainfall in the future climate than GCMs downscaled by CCLM4 model.

In some cases bias correction methods showed poor representation of extreme climatic and hydrologic values (Maraun, 2012; Wang and Kotamarthi (2015); Liersch et al. (2016). For instance, Liersch et al., (2016) investigated weakness of bias correction techniques in reproducing high and low streamflow and deterioration of hydrological simulation by bias correction techniques. This could be the inaccuracy of the bias correction methods in developing scale and shape parameters which impact the distribution and intensity of climatic and hydrological values. In this study, the selected bias correction technique i.e distribution mapping technique was effective in adjusting the 90th percentile and wet day probability of RCMs simulation with observed counterparts (Fig. 6b). The RCMs before and after bias correction consistently showed a decrease of rainfall and an increase in temperature, which mean bias correction triggers no change in climate change signal.

In hydrological modelling, P-factor (95PPU) and the r-factor ^{measure} input uncertainty, conceptual model uncertainty and parameter uncertainty (Abbaspour et al., 2007). This study showed good performance of P-factor and the r-factor, however, only 64%-80% of the observed data was bracketed by the 95PPU. This accentuates the observed streamflow data is not high quality (Abbaspour et al., 2007) and contains some outliers. For instance, in the year 1994, high observed discharge is recorded and the 95PPU did not bracketed such

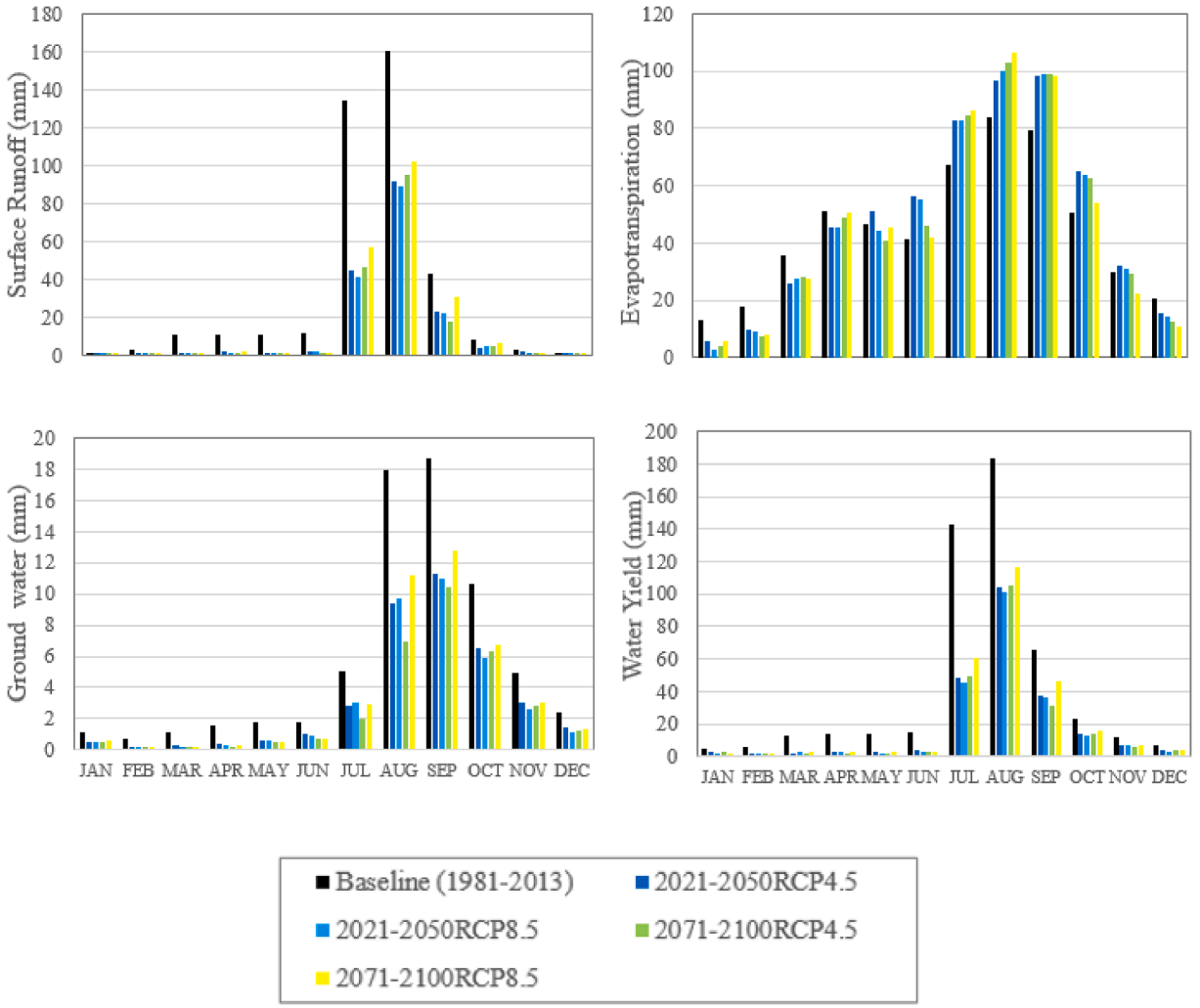

Fig. 14. Mean monthly distribution of the hydrologic components for baseline, the near term (2021–2050) and long-term (2071–2100) climate scenarios.

like high flows. In general, this study provides a comprehensive understanding of the hydrology of the basin and the response of hydrological components to different climate scenarios for the stakeholders of the basin and the policymakers.

4. Conclusion

The livelihood of the inhabitants of the Jemma sub-basin is highly dependent on rain-fed agriculture. On the other hand, the rain-fed agriculture is frequently affected by climate change and variability. Since rainfall is the main source of water yield of the Jemma sub-basin, a change in climate could trigger repercussion on the water resources of the basin. This study used bias adjusted ensemble mean of RCM simulations (E-RCM), single RCM simulation (E-RCM) and the SWAT model to explore impact of climate change on the water balance components of the Jemma sub-basin using the SWAT model. Multi-site calibration and validation of the model reproduced the baseline hydrological conditions of the sub-basin. The sensitivity analysis showed that streamflow is highly sensitive to parameters related to surface water processes. A strong relationship was found among rainfall, surface runoff and total water yield both spatially and seasonally.

This study used bias adjusted ensemble mean of RCM simulations (E-RCM) and single RCM simulation (E-RCM) to explore hydrological climate change impact. Ensemble mean of RCM simulations and single RCM simulation revealed comparable climate change signal. This indicates low uncertainty between the RCMs in the ensemble mean and single RCM simulation. However, this study recommends to use the ensemble mean which can capture under and over estimation of single RCM simulation. In fact other studies (Bates et al., 2008; Teutschbein and Seibert, 2010; IPCC, 2013) also suggest ensemble mean of RCM simulations for climate to change impact assessment that single RCM simulation.

A decrease in rainfall and an increase in temperature and evapotranspiration will cause a decrease in surface runoff and water yield

Table 8
Mean seasonal rainfall (mm) under baseline and future climate scenarios. The outputs of the water balance components were estimated for an ensemble mean of RCMs under RCP4.5 and RCP8.5 emission scenarios.

	Baseline (1981– 2013)	Near-term 2021–2050 (RCP4.5)	Near-term 2021–2050 (RCP8.5)	Long-term 2071–2100 (RCP4.5)	Long-term 2071–2100 (RCP8.5)
ET(mm yr^{-1})					
Summer (June – September)	271.83	333.89(23%)	337.01(24%)	332.26(22%)	332.48(22.3%)
Spring (March-May)	133.86	122.29(-9%)	116.76(-13%)	117.43(-12%)	123.90(-7.4%)
Winter(December–February)	51.32	30(-41%)	26.20(-49%)	23.64(-54%)	24.34(-53%)
SURQ (mm yr^{-1})					
Summer (June – September)	362.49	172.86(-54%)	166.26(-56%)	172.24(-54.3%)	203.52(-45%)
Spring (March-May)	37.53	8.69(-89%)	8.98(-88%)	7.90(-91%)	9.69(-86%)
Winter(December–February)	8.49	3.28(-77%)	3.99(-82%)	4.53(-72%)	4.68(-69%)
GWQ (mm yr^{-1})					
Summer (June – September)	43.50	24.54 (-44%)	24.69 (-43%)	20.16 (-54%)	27.52 (-37%)
Spring (March-May)	4.44	1.24 (-72%)	1.18 (-73%)	0.88 (-80%)	0.97 (-78%)
Winter(December–February)	4.22 ()	2.18 (-48%)	1.82 (-57%)	1.97 (-53%)	2.15 (-49%)
WYLD (mmyr^{-1})					
Summer (June – September)	406.76	194(-52%)	186.11(-54%)	188.72(-54%)	226.36(-44%)
Spring (March-May)	41.69	7.62(-82%)	7.39(-82.3%)	6.15(-85%)	7.96(-81%)
Winter(December–February)	17.35	8.41(-52%)	7.07(-59%)	7.84(-55%)	8.45(-51%)

Table 9
Mean annual water balance components under baseline and future climate scenarios. The changes in the water balance components were estimated for CCLM4 (MPI-ESM-LR) model under RCP4.5 and RCP8.5 emission scenarios.

	Baseline (1981– 2013)	2021–2050 (RCP4.5)	2021–2050 (RCP8.5)	2071–2100 (RCP4.5)	2071–2100 (RCP8.5)
Rainfall (mm yr^{-1})	1039.00	828 (-18%)	808(-20%)	782(–22%)	804 (-20%)
ET(mm yr^{-1})	537.30	567.42 (7%)	561(4.4%)	559(4%)	558(4%)
SURQ (mm yr^{-1})	419.33	232.46(-47%)	213.67(-51%)	201.84(-54%)	206.34(-53%)
GWQ (mm yr^{-1})	67.81	39.82(-41%)	37.68(-44%)	35.35(-48%)	36.25(-46%)
LATQ(mm yr^{-1})	15.59	11.24(-28%)	9.45(-39%)	8.78(-44%)	9.47(-39%)
WYLD (mmyr^{-1})	500.84	265.53(-47%)	250.8(-50%)	235.97(-53%)	242.06(-52%)
PERC(mmyr^{-1})	86.12	58.373(–32%)	51.62(-40%)	47.66(-45%)	50.36(-41%)

Table 10
Trend of TMAX under baseline and future climate scenarios in different climatic stations of the Jemma sub-basin.

Stations	Surface runoff		Actual evapotranspiration		Total water yield		Groundwater	
	Zs	b_{sen}	Zs	b_{sen}	Zs	b_{sen}	Zs	b_{sen}
Baseline (1983–2013)	1.28	1.98	0.21	1.78	1.46	2.78	*2.42*	*0.82*
RCP4.5 (2021–2050	−0.07	−0.09	0.19	1.48	−0.21	−0.23	***−0.64***	***−0.17***
RCP8.5 (2021–2050)	*−1.00*	**−1.06***	0.29	1.53*	***−0.50***	−0.60	−2.00	−0.41
RCP4.5 (2071–2100)	*−0.37*	**−0.35***	0.22	1.66	−0.63	−0.72	−0.88	−0.16
RCP8.5 (2071–2100)	−0.50	−0.52	0.24	1.49*	−0.13	−0.17	−0.83	−0.23

Zs and b_{sen} are Mann-Kendal test and Sen Slope values respectively.
*Statistically significant trends at the 5% significance level.

under different future climate scenarios. There is no strong seasonal shift of rainfall, runoff and water yield between the current and projected future climate conditions. The highest decrease in water yield may be observed during the rainy season (June-September) suggesting that the rainfed agricultural production will be severely impacted. This rainy season is the main agricultural cultivation season, as a result a decline on rainfall and water yield will decrease crops growing season, soil water for crops, crops productivity and water availability to livestock and other domestic uses.

Climate change and its hydrologic impact in the Jemma sub-basin prompts to implement sustainable surface water resource management strategies. To avert future climate change impact on each sub-watershed of the sub-basin, surface runoff management alternatives would be essential to maintain water availability, since surface runoff contributes large proportion to the total water yield. To develop surface water resource management strategies, the projected climate change scenarios and the simulated impacts of climate change are to be incorporated in the adaptation decisions analysis. Such strategies may provide optimal benefits in maintaining the water resources availability, to mitigate and adapt adverse impacts of climate conditions and thereby maintain or even enhance agricultural production. However, a detailed study is warranted to identify water management technologies that suits the biophysical and socio-economic conditions in the Jemma sub-basin.

Declaration of Competing Interest

The authors declare that they have no known competing financial interests or personal relationships that could have appeared to influence the work reported in this paper.

Acknowledgement

This study was made possible through financial support to the first author from Debretabor University of Ethiopia. The International Foundation for Science (Grant No. W_6227-1) also funded this study. We are also thankful to the Ethiopian National Meteorological Agency and the Ministry of Water, Irrigation and Electricity of Ethiopia, which kindly provided us the daily weather data and hydrologic data.

References

Abbaspour, K.C., 2015. SWAT CUP SWATCalibration and Uncertainty Programs. A User Manual.
Abbaspour, K.C., Johnson, C.A., van Genuchten, M.T., 2004. Estimating Uncertain Flow and Transport Parameters Using a Sequential Uncertainty Fitting Procedure. Vadose Zone J. 3 (4), 1340–1352.
Abbaspour, K.C., Yang, J., Maximov, I., Siber, R., Bogner, K., Mieleitner, J., Zobrist, J., Srinivasan, R., 2007. Modelling hydrology and water quality in the pre-alpine/alpine Thur watershed using SWAT. J. Hydrol. 333 (2-4), 413–430.
Adem, A.A., Tilahun, S.A., Ayana, E.K., Abeyou W. Worqlul, T.T., Melesse, A., Dessu, S.B., M, A., 2016. Climate Change Impact on Stream Flow in the Upper Gilgel Abay Catchment, Blue Nile basin, Ethiopia. Landscape Dynamics, Soils and Hydrological Processes in Varied Climates v–vi. https://doi.org/10.1007/978-3-319-18787-7.
ALI, Y.S.A., CROSATO, A., MOHAMED, Y.A., ABDALLA, S.H., WRIGHT, N.G., 2014. Sediment balances in the Blue Nile River Basin. Int. J. Sedim. Res. 29 (3), 316–328.

Amsalu, A., Stroosnijder, L., Graaff, J.d., 2007. Long-term dynamics in land resource use and the driving forces in the Beressa watershed, highlands of Ethiopia. J. Environ. Manage. 83 (4), 448–459.
Arnell, N.W., 2004. Climate change and global water resources : SRES emissions and socio-economic scenarios 14, 31–52. https://doi.org/10.1016/j.gloenvcha.2003.10.006.
Arnold, J., Kiniry, J., Srinivasan, R., Williams, J., Haney, E., Neitsch, S., 2012. Soil & Water Assessment Tool: Input/Output Documentation Version 2012.
Arnold, J.G., Moriasi, D.N., Gassman, P.W., Abbaspour, K.C., White, M.J., Srinivasan, R., Santhi, C., Harmel, R.D., van Griensven, A., Liew, M.W.V., Kannan, N., Jha, M.K., 2012b. SWAT: Model Use, Calibration, and Validation. Am. Soc. Agri. Biol. Eng. 55, 1491–1508.
Arnold, J.G., Srinivasan, R., Muttiah, R.S., Williams, J., 1998. Large area hydrologic modeling and assessment part I: model development. J. Am. Water Resour. Assoc. 34, 73–89. https://doi.org/10.1016/S0899-9007(00)00483-4.
Bastola, S., Misra, V., 2013. Evaluation of dynamically downscaled reanalysis precipitation data for hydrological application. Hydrol. Process. https://doi.org/10.1002/hyp.9734.
B. Bates Z. Kundzewicz S. Wu J. Palutikof Climate change and water 2008.
Begou, J.C., Jomaa, S., Benabdallah, S., Bazie, P., Afouda, A., Rode, M., 2016. Multi-Site Validation of the SWAT Model on the Bani Catchment : Model Performance and. Water 178, 1–23. https://doi.org/10.3390/w8050178.
Betrie, G.D., Mohamed, Y.A., van Griensven, A., Srinivasan, R., 2012. Sediment management modelling in the Blue Nile Basin using SWAT model Hydrol. Earth Syst. Sci. 15 (3), 807–818. https://doi.org/10.5194/hess-15-807-2011. https://hess.copernicus.org/articles/15/807/2011/.
Beyene, T., Lettenmaier, D.P., Kabat, P., 2010. Hydrologic impacts of climate change on the Nile River Basin: implications of the 2007 IPCC scenarios. Clim. Change 100, 433–461. https://doi.org/10.1007/s10584-009-9693-0.
Bhatta, B., Shrestha, S., Shrestha, P.K., Talchabhadel, R., 2019. Evaluation and application of a SWAT model to assess the climate change impact on the hydrology of the Himalayan River Basin. CATENA 181, 104082. https://doi.org/10.1016/j.catena.2019.104082.
Cao, W., Bowden, W.B., Davie, T., Fenemor, A., 2006. Multi-variable and multi-site calibration and validation of SWAT in a large mountainous catchment with high spatial variability. Hydrol. Process. 20 (5), 1057–1073.
Chaemiso, S.E., Abebe, A., Pingale, S.M., 2016. Assessment of the impact of climate change on surface hydrological processes using SWAT: a case study of Omo-Gibe river basin, Ethiopia. Model. Earth Syst. Environ. 2 (4), 1–15.
Conway, D., Schipper, E.L.F., 2011. Adaptation to climate change in Africa : Challenges and opportunities identified from Ethiopia. Global Environ. Change 21, 227–237. https://doi.org/10.1016/j.gloenvcha.2010.07.013.
Dile, Y.T., Berndtsson, R., Setegn, S.G., 2013. Hydrological Response to Climate Change for Gilgel Abay River , in the Lake Tana Basin - Upper Blue Nile Basin of Ethiopia. PLoS ONE 8, 12–17. https://doi.org/10.1371/journal.pone.0079296.
M.E. Elshamy I.A. Seierstad A. Sorteberg Impacts of climate change on Blue Nile flows using bias-corrected GCM scenarios Hydrol. Earth Syst. Sci. 13 5 551 565 10.5194/hess-13-551-2009 https://hess.copernicus.org/articles/13/551/2009/.
G.H. Fang J. Yang Y.N. Chen C. Zammit Comparing bias correction methods in downscaling meteorological variables for a hydrologic impact study in an arid area in China Hydrol. Earth Syst. Sci. 19 6 2547 2559 10.5194/hess-19-2547-2015 https://hess.copernicus.org/articles/19/2547/2015/.
FAO, IIASA, ISRIC, ISS-CAS, JRC, . FAO, Rome, Italy and IIASA, Laxenburg, Harmonized World Soil Database (version 1.0) 2008 Austria.
Feyissa, G., Gete, Z., Woldeamlak, B., Gebremariam, E., 2018. Downscaling of Future Temperature and Precipitation Extremes in Addis Ababa under Climate Change. https://doi.org/10.3390/cli6030058.
Gebrehiwot, S.G., Ilstedt, U., 2011. Hydrological characterization of watersheds in the Blue Nile Basin , 11–20. https://doi.org/10.5194/hess-15-11-2011.
Geleta, C.D., Gobosho, L., 2018. Climate Change Induced Temperature Prediction and Bias Correction in Finchaa Watershed 18, 324–337. https://doi.org/10.5829/idosi.aejaes.2018.324.337.
A. van Griensven P. Ndomba S. Yalew F. Kilonzo Critical review of SWAT applications in the upper Nile basin countries Hydrol. Earth Syst. Sci. 16 9 3371 3381 10.5194/hess-16-3371-2012 https://hess.copernicus.org/articles/16/3371/2012/.
Gudmundsson, L., Bremnes, J.B., Haugen, J.E., Engen-Skaugen, T., 2012. Technical Note: Downscaling RCM precipitation to the station scale using statistical transformations – A comparison of methods. Hydrol. Earth Syst. Sci. 16, 3383–3390. https://doi.org/10.5194/hess-16-3383-2012.
Stefan Hagemann Cui Chen Jan O. Haerter Jens Heinke Dieter Gerten Claudio Piani Impact of a Statistical Bias Correction on the Projected Hydrological Changes Obtained from Three GCMs and Two Hydrology Models 12 4 2011 556 578.
Hailemariam, K., 1999. Impact of climate change on the water resources of Awash River Basin, Ethiopia. Clim. Res. 12, 91–96.
Hurni, H., Tato, K., Zeleke, G., 2005. The Implications of Changes in Population , Land Use , and Land Management for Surface Runoff in the Upper Nile Basin Area of Ethiopia The Implications of Changes in Population , Land Use , and Land Management for Surface Runoff in the Upper Nile Basin Ar. https://doi.org/10.2307/3674675.
IPCC Climate Change 2013: The Physical Science Basis. Working Group I Contribution to the Fifth Assessment Report of the Intergovernmental Panel on Climate Change 2013.
Kendall, M., 1975. Rank Correlation Measures. Charles Griffin, London.
Liersch, S., Tecklenburg, J., Rust, H., Dobler, A., Fischer, M., Kruschke, T., Koch, H., Hattermann, F.F., 2016. Are we using the right fuel to drive hydrological models ? A climate impact study in the Upper Blue Nile. Hydrol. Earth Syst. Sci. Discuss 1–34. https://doi.org/10.5194/hess-2016-422.
Mann, H., 1945. Nonparametric tests against trend. Econometrica 13 (3), 245–259.
Maraun, D., 2012. Nonstationarities of regional climate model biases in European seasonal mean temperature and precipitation sums. Geophys. Res. Lett. 39, 1–5. https://doi.org/10.1029/2012GL051210.
Mehan, Sushant, Aggarwal, Ruchir, Gitau, Margaret W., Flanagan, Dennis C., Wallace, Carlington W., Frankenberger, Jane R., 2019. Assessment of hydrology and nutrient losses in a changing climate in a subsurface-drained watershed. Sci. Total Environ. 688, 1236–1251.
Mehan, S., Kanan, N., Neupane, R., McDaniel, R., Kumar, S., 2016. Climate Change Impacts on the Hydrological Processes of a Small Agricultural Watershed. Climate 4, 56. https://doi.org/10.3390/cli4040056.
Mekonnen, D.F, Disse, M., 2016. Analyzing the future climate change of Upper Blue Nile River Basin (UBNRB) using statistical down scaling techniques. Hydrol. Earth Syst. Sci. Discuss 1–27. https://doi.org/10.5194/hess-2016-543.
Moriasi, D.N., Gitau, M.W., Pai, N., Daggupati, P., 2015. Hydrologic and Water Quality Models: Performance Measures and Evaluation Criteria. Trans. ASABE 58, 1763–1785.
Moriasi, D.N., Arnold, J.G., Liew, M.W. Van, Bingner, R.L., Harmel, R.D., Veith, T.L., 2007. Model evaluation guidelines for systematic quantification of accuracy in watershed simulations. Am. Soc. Agri. Biol. Eng. 50, 885–900.
Moss, Richard H., Edmonds, Jae A., Hibbard, Kathy A., Manning, Martin R., Rose, Steven K., van Vuuren, Detlef P., Carter, Timothy R., Emori, Seita, Kainuma, Mikiko, Kram, Tom, Meehl, Gerald A., Mitchell, John F.B., Nakicenovic, Nebojsa, Riahi, Keywan, Smith, Steven J., Stouffer, Ronald J., Thomson, Allison M., Weyant, John P., Wilbanks, Thomas J., 2010. The next generation of scenarios for climate change research and assessment. Nature 463 (7282), 747–756.
Muerth, M.J., Gauvin St-Denis, B., Ricard, S., Velázquez, J.A., Schmid, J., Minville, M., Caya, D., Chaumont, D., Ludwig, R., Turcotte, R., 2013. On the need for bias correction in regional climate scenarios to assess climate change impacts on river runoff. Hydrol. Earth Syst. Sci. 17, 1189–1204. https://doi.org/10.5194/hess-17-1189-2013.
Nash, J.E., Sutcliffe, J.V., 1970. Riverflow forecasting through conceptualmodels: part 1. dA discussion of principles. J. Hydrol. 10, 282–290.
NMA, 2007. Climate Change National Adaptation Programme of Action (NAPA) of Ethiopia.
Olsson, J., Arheimer, B., Borris, M., Donnelly, C., Foster, K., Nikulin, G., Persson, M., Perttu, A.-M., Uvo, C., Viklander, M., Yang, W., 2016. Hydrological Climate Change Impact Assessment at Small and Large Scales: Key Messages from Recent Progress in Sweden. Climate 4, 39. https://doi.org/10.3390/cli4030039.
Pohlert, T., 2016. Package 'trend'; Title Non-Parametric Trend Tests and Change-Point Detection.
Saha, S., Moorthi, S., Pan, H., Wu, X., Wang, J., Nadiga, S., 2010. The NCEP Climate Forecast System Reanalysis. Am. Meteorol. Soc. 1015–1057.

Santhi, C., Kannan, N., Arnold, J.G., Luzio, M. Di, 2009. Spatial calibration and temporal validation of flow for regional scale hydrologic modeling. J. Am. Water Resour. Assoc. 44, 829–846. https://doi.org/10.1111/j.1752-1688.2008.00207.x.

Sen, Pranab Kumar, 1968. Estimates of the Regression Coefficient Based on Kendall's Tau. J. Am. Stat. Assoc. 63 (324), 1379–1389.

Setegn, S.G., Rayner, D., Melesse, A.M., Dargahi, B., Srinivasan, R., 2011. Impact of climate change on the hydroclimatology of Lake Tana Basin, Ethiopia. Water Resour. Res. 47, 1–13. https://doi.org/10.1029/2010WR009248.

Setegn, Shimelis G., Srinivasan, Ragahavan, Melesse, Assefa M., Dargahi, Bijan, 2009. SWAT model application and prediction uncertainty analysis in the Lake Tana Basin, Ethiopia. Hydrol. Process. n/a–n/a. https://doi.org/10.1002/hyp.7457.

Soliman, E.S.A., Sayed, M.A.A., Jeuland, M., 2009. Impact Assessment of Future Climate Change for the Blue Nile Basin, Using a RCM Nested in a GCM. Nile Basin Water Engin. Sci. Mag. 2, 15–30.

Taye, M.T., Dyer, E., Hirpa, F.A., Charles, K., 2018. Climate change impact on water resources in the Awash basin, Ethiopia. Water 10, 1–16. https://doi.org/10.3390/w10111560.

Teutschbein, Claudia, Seibert, Jan, 2012. Bias correction of regional climate model simulations for hydrological climate-change impact studies: Review and evaluation of different methods. J. Hydrol. 456-457, 12–29.

Teutschbein, C., Seibert, J., 2010. Regional Climate Models for Hydrological Impact Studies at the Catchment Scale : A Review of Recent Modeling. Strategies 7, 834–860.

The R Core Team, 2015. R: A Language and Environment for Statistical Computing. R Foundation for Statistical Computing.

Wang, J., Kotamarthi, V.R., 2015. High-resolution dynamically downscaled projections of precipitation in the mid and late 21st century over North America. Earth's Future 3, 268–288. https://doi.org/10.1002/2015EF000304.Received.

Wang, Weiguang, Sun, Fengchao, Luo, Yufeng, Xu, Junzeng, 2012. Changes of Rice Water Demand and Irrigation Water Requirement in Southeast China under Future Climate change. Procedia Eng. 28, 341–345.

Worku, G., Teferi, E., Bantider, A., Dile, Y.T., 2018a. Observed changes in extremes of daily rainfall and temperature in Jemma Sub-Basin, Upper Blue Nile Basin, Ethiopia. Theoretical and Applied Climatology 135, 839–854. https://doi.org/10.1007/s00704-018-2412-x.

Worku, G., Teferi, E., Bantider, A., Dile, Y.T., 2019. Statistical bias correction of regional climate model simulations for climate change projection in the Jemma sub-basin, upper Blue Nile Basin of Ethiopia. Theor. Appl. Climatol. 139 (3–4), 1569–1588.

Worku, Gebrekidan, Teferi, Ermias, Bantider, Amare, Dile, Yihun T., Taye, Meron Teferi, 2018b. Evaluation of regional climate models performance in simulating rainfall climatology of Jemma sub-basin, Upper Blue Nile Basin, Ethiopia. Dyn. Atmos. Oceans 83, 53–63.

World Bank, 2006. Managing Water Resources to Maximise Sustainable Growth: A Country Water Resources Assistance Strategy for Ethiopia. World Bank, Washington, DC.

Worqlul, A.W., Taddele, Y.D., Ayana, E.K., Jeong, J., 2018. Impact of climate change on streamflow hydrology in Headwater Catchments of the upper Blue Nile. Water 10 (120). https://doi.org/10.3390/w10020120.

Yilma, A.D., Awulachew, S.B., 2009. Characterization and Atlas of the Blue Nile Basin and its Sub basins. International Water Management Institute.

Zhang, X., Srinivasan, R., Van Liew, M., 2008. Multi-site calibration of the SWAT model for hydrologic modeling. Trans. ASABE 51, 2039–2049.